Articles in PresS. J Neurophysiol (May 9, 2007). doi:10.1152/jn.00252.2007

Dissociation of eye and head components of gaze shifts by stimulation of the omnipause neuron region

Neeraj J. Gandhi [1, 2]
David L. Sparks [2]

[1] Departments of Otolaryngology, Neuroscience and Bioengineering
Center for the Neural Basis of Cognition
University of Pittsburgh, PA 15213

[2] Department of Neuroscience
Baylor College of Medicine
Houston, TX 77030

Address correspondences to:
Neeraj J. Gandhi, Ph.D.
203 Lothrop Street
Eye and Ear Institute, Room 108
University of Pittsburgh
Pittsburgh, PA 15213

Email: neg8@pitt.edu
Voice: (412) 647-3076
Fax: (412) 647-0108

ABSTRACT

Natural movements often include actions integrated across multiple effectors. Coordinated eye-head movements are driven by a command to shift the line of sight by a desired displacement vector. Yet, because extraocular and neck motoneurons are separate entities, the gaze shift command must be separated into independent signals for eye and head movement control. We report that this separation occurs, at least partially, at or before the level of pontine omnipause neurons (OPNs). Stimulation of the OPNs prior to and during gaze shifts temporally decoupled the eye and head components by inhibiting gaze and eye saccades. In contrast, head movements were consistently initiated before gaze onset, and ongoing head movements continued along their trajectories, albeit with some characteristic modulations. After stimulation offset, a gaze shift composed of an eye saccade and a reaccelerated head movement was produced to preserve gaze accuracy. We conclude that signals subject to OPN inhibition produce the eye movement component of a coordinated eye-head gaze shift and are not the only signals involved in the generation of the head component of the gaze shift.

INTRODUCTION

We interact with our environment by generating actions coordinated across multiple effector systems. Integrated movements of the eyes, head, torso and/or limbs are used to perform activities such as driving a car (Land 1992), hitting a ball (Land and McLeod 2000), or even generating defensive postures (Graziano et al. 1997). Studies probing the neural bases of integrated motor control have typically considered the coordination of oculomotor subsystems (Fukushima et al. 2002; Gardner and Lisberger 2001; Keller et al. 1996; Walton and Mays 2003) or of eye movements with skeletal effectors like the head (Crawford et al. 2003; Guitton et al. 2003; Pélisson et al. 2003) and the hand (Cohen and Andersen 2002; Courjon et al. 2004; Crawford et al. 2004; Stuphorn et al. 2000).

Reorienting the line of sight is often accomplished by coordinated eye-head movements (Bizzi et al. 1971). In general, the saccadic eye and head components are temporally coupled (Freedman and Sparks 1997b; Phillips et al. 1995; Zangemeister and Stark 1982a); the saccadic eye component initiates the gaze shift and the onset of the head movement lags behind, at least in part, because of its heavier inertial load. When the initial eye-in-head position is deviated in the direction of the gaze shift (Becker and Jürgens 1992; Freedman and Sparks 1997b; Fuller 1996) or when the location and timing of the stimulus are predictable (Bizzi et al. 1972; Moschner and Zangemeister 1993; Zangemeister and Stark 1982a; b), however, the lag in the head component can be reduced or it can even lead gaze onset. Furthermore, long duration, sub-threshold microstimulation of the superior colliculus, a structure believed to issue a desired gaze displacement command (Freedman and Sparks 1997a; Freedman et al. 1996; Klier et al. 2001), can evoke a head-only movement – the eyes counter-rotate in the orbits – or a

head-only movement that precedes the onset of the gaze shift (Corneil et al. 2002; Pélisson et al. 2001). Thus, the timing of head initiation relative to gaze onset need not be rigidly constrained.

Independent control of the eyes and head occurs naturally at the level of the extraocular and neck motoneurons, although some form of separate processing has also been proposed to occur in cortical (Chen 2006; Chen and Walton 2005; Constantin et al. 2004; Constantin et al. 2006), subcortical (Gandhi and Walton 2006; Pathmanathan et al. 2005a; Pathmanathan et al. 2005b; Walton and Gandhi 2006), and cerebellar (Quinet and Goffart 2005) structures. It has been hypothesized that head movements associated with gaze shifts are driven by at least two parallel pathways: one is gated by the pontine omnipause neurons (OPNs) and issues movement commands to the eyes and head, and the other bypasses the OPN gate and does not encode a saccadic eye movement command (Corneil et al. 2002; Galiana and Guitton 1992; Goossens and Van Opstal 1997; Guitton et al. 1990). The objective of the present study was to test the functional contribution of head pathway(s) external to the OPN inhibition. Microstimulation was delivered to the OPN region either prior to or at the onset of horizontal head-unrestrained gaze shifts directed to the location of a briefly flashed target. Given that the OPNs inhibit excitatory burst neurons (Curthoys et al. 1984) that project to the abducens motoneurons, it was expected that the microstimulation would prevent generation of the saccadic eye component of gaze shifts. The key additional predictions were: (1) initiation of a head movement would consistently precede the gaze shift when microstimulation was delivered before gaze onset; and (2) an ongoing head movement would continue along its trajectory when stimulation was triggered after gaze onset.

Preliminary versions of this data have been published previously (Gandhi and Sparks 2001a, 2000; Sparks et al. 2001; Sparks and Gandhi 2003).

METHODS

General procedures

Two juvenile rhesus monkeys (*Macaca mulatta*) weighing 5-8 kg served as subjects. All experimental protocols were approved by the Institute Animal Care and Use Committee at the Baylor College of Medicine and complied with the guidelines of the Public Health Service policy on Humane Care and Use of Laboratory Animals. All surgical procedures were performed in a sterile environment and under isofluorane anesthesia. Using Vetbond tissue adhesive, a search coil was attached to the sclera of one eye of each monkey. Another coil, a head-restraint post, and a stainless steel chamber were secured to the skull. The cylinder was slanted laterally in the frontal plane at an angle of 26° so that a microelectrode penetration through its center would reach the midline in the inter-aural plane 1-mm below inter-aural zero.

Post recovery, the animal was trained to sit in a customized chair fitted with neck, waist and chest plates that minimized (approximately ±10°) but did not prevent trunk and body movements. On each experimental day, the chair with the animal inside it was carted to the laboratory. A micro-miniature laser (Edmund Optics, Inc.; Barrington, NJ) was attached to the animal's head implant. In addition, a hydraulic microdrive was secured to the chamber and a parylene coated tungsten microelectrode (Micro Probe, Inc; Gaithersburg, MD) was inserted into the brain. The animal with its chair were then placed in a magnetic field frame (CNC Engineering; Seattle, WA). Electromagnetic

induction technique was used to measure eye-in-space (gaze) and head-in-space positions from the coils around the eye and in the head implant, respectively. Eye-in-head position was computed as the difference of gaze and head positions. See Gandhi and Sparks (2001b) for more details.

Experimental setup and behavioral tasks

When seating in the magnetic field frame, the animal faced a flat visual display consisting of 41 rows and 49 columns of tri-state light emitting diodes (LEDs) that could light up red, green or yellow. It was placed 72 cm from the center of the field coil, which corresponds to inter-LED spacing of 2° on a tangential plane. Maximum target eccentricity, with respect to straight ahead, was ±48° horizontally and ±40° vertically. All target eccentricities reported in this manuscript are in tangential coordinates and can be transformed into rotational coordinates, as described previously (Gandhi and Sparks 2001b; Huebner et al. 1995).

While the electrode was being lowered into the PPRF region, the animal performed two randomly interleaved behavioral tasks. At the onset of each trial, a red LED and the micro-miniature laser were illuminated. When turned on, the laser module emitted a red beam of light onto the visual display panel. The animal was granted 2000 ms to both fixate the red target and align the laser beam (i.e., the head) inside an imaginary, computer-controlled window (radius: 4°-6°) around the LED location, and then maintain these requirements for 700-1000 ms. At the end of this step, the eyes are approximately centered in the orbits, and gaze and head positions are nearly equivalent. The remainder of the steps was dependent on the ensuing behavioral task.

In the *memory-guided* gaze shift task, a gaze target (yellow LED) was flashed for 500-1300 ms, while the head target (red LED) and miniature laser remained on. Another 500-900 ms after the offset of gaze target, the laser and red LED were extinguished, which cued the monkey to initiate a gaze shift. If gaze position reached within an imaginary, computer-controlled window (radius: 6°-10°) around the flashed target location in ≤500 ms, the LED was re-illuminated, and a final fixation of 1500-2000 ms triggered delivery of a liquid reward. A relatively large window size was necessary to account for the variability of endpoints for movements made in the dark (Goffart et al. 2006; White et al. 1994) and for greater hypometria associated with large movements (Becker 1991).

In the *gap* gaze shift task, the LED and the laser were extinguished after alignment of the head and gaze with the red target. Following a gap of 200-500 ms, during which neither fixation condition could be violated, a gaze (yellow) target was illuminated at an eccentricity of 40°-60° and remained on until the end of the trial. The monkeys were allowed 800 ms to direct gaze into a computer-controlled window (radius: 6°-10°) around the yellow target location. To allow completion of the head movement, a final fixation of 1500-2000 ms was required before a liquid reward was delivered. A window constraint was not placed on the head position signal during acquisition of the gaze target.

Stimulation trials were introduced once the electrode penetration entered the PPRF region of the brain stem and OPNs were identified based on their discharge characteristics (cf. (Gandhi and Keller 1999)). The initial objective was to optimize the microelectrode location within the OPN region. On a subset of the gap trials (25-50%),

microstimulation (10-30 μA, 200-300 Hz, 100-300 ms, 0.25 ms duration cathode pulses) was applied to the OPN region 100-200 ms after the offset of the red LED and laser. The gaze target was illuminated after the offset of the stimulation, and the animals were rewarded for acquiring the gaze target. If the tip of the stimulation electrode was located on the fringe of the OPN area where stimulation produces a constant velocity gaze movement (Cohen and Komatsuzaki 1972), the electrode was moved to eliminate this effect. This positioning effort also served to minimize stimulation-induced activation effects of nearby pathways (e.g., reticulospinal, tectospinal, and interstitiospinal) on head movement generation.

Upon satisfactory positioning of the electrode, trials with stimulation triggered during the gap period were reduced to ~5% of all trials, but other stimulation tasks were introduced. On a subset of the trials, microstimulation (10-30 μA, 200-300 Hz, 100-300 ms, 0.25 ms duration cathode pulses) was triggered on gaze onset, which actually was detected online as deviation of either gaze or head position outside of its respective computer-controlled window constraint. On another fraction of interleaved trials, the microstimulation was delivered 100-200 ms after the cue to initiate the gaze shift (target onset in the gap task and fixation point offset in the memory-guided gaze shift task). This trial type was designed to test whether and how the latencies of gaze and head movements are compromised by OPN stimulation prior to gaze onset. In this latter condition, if stimulation onset followed gaze onset, the trial was relocated to the "stimulation triggered on gaze onset" database. For both stimulation trials, the gaze target was extinguished with the onset of the stimulation. If gaze position reached within an imaginary, computer-controlled window (radius: 6°-10°) around the gaze target

location in ≤500 ms after stimulation offset, the LED was re-illuminated, and a final fixation of 1500-2000 ms triggered a liquid reward.

In general, stimulation within the context of gap trials was more common at the beginning of each experimental day, as the electrode position within the OPN region was being fine tuned. Upon satisfactory placement of the electrode, the memory-guided gaze shift task, with and without stimulation, constituted approximately 75-80% of all trials. The rest of the trials were composed of the gap task with and without stimulation. Collectively, stimulation was delivered in 25-40% of all trials. Stimulation parameters were kept constant within a block of trials, irrespective of whether the current was injected before or after gaze onset. We typically only modified the stimulation duration in between blocks, when we felt it was necessary to prolong the stimulation-induced interruption to better visualize the effect of stimulation on the head component of the gaze shift. For the analyses, however, we did not parse the data according to stimulation duration as we did not consistently have enough trials for a specific stimulation duration and the same target configuration (as described below).

A qualitative assessment indicated that stimulation produced similar effects on both gap and memory-guided gaze shift trials and hence the data were pooled. Control data for the two trials types were also combined, as our gap trials did not produce an appreciable number of express latency gaze shifts. This is most likely due to factors such as small percentage of gap trials, variable gap durations and numerous target locations.

All target configurations required horizontal gaze shifts. The vertical eccentricity of all targets was 0° and, based on visual inspection, at eye level. Typically, the initial red LED was presented at 0°, +20° (right visual field) or –20° (left visual field), and the

yellow, gaze target appeared at ±40° or ±60° with respect to the initial target. If the gaze target location was beyond the visual display boundary, the most distal target (±48°) was illuminated to prevent any bias the animal might develop to evoke centripetal gaze shifts when the initial head and gaze positions were directed away from the midline. Gaze shifts directed to targets illuminated at 40° and 48° in the same hemifield were combined. Trials in which both initial and gaze targets were presented in the same hemifield (e.g., from 20° right to 40° right) were excluded from analysis.

Data acquisition and analyses

Data were sampled at 500 Hz using in-house software. Data were analyzed off-line using in-house software and Matlab (The Mathworks, Inc., Natick, MA). Typically, velocity criteria were used to detect the onset and offset of gaze, eye and head movements. For gaze and eye movements, the onset and offset velocity thresholds were 80°/sec and 60°/sec, respectively. For head movements, the onset and offset velocity thresholds were 8°/sec and 5°/sec, respectively.

The majority of the analyses presented in the manuscript required computing static parameters (latency, amplitude, magnitude and time of peak head velocity and acceleration) and comparing them between control and stimulation conditions. In general, the Wilcoxon rank sum test – equivalently, the Mann-Whitney *U* test – that compares the medians of the distributions of control and stimulation conditions was used to test for statistical significance. When appropriate (and as indicated in the Results), a pair-wise comparison was performed with the Wilcoxon sign rank test of equality of medians across matched samples of control and stimulation trials. For comparison,

analogous *t*-tests were also performed and comparable results were obtained. Additionally, a two-way ANOVA test was performed to determine whether any changes observed in the static parameters listed above could be statistically related to initial head position (center or contralateral) or trial condition (stimulation or control).

A dynamics analysis was used to test the null hypothesis that stimulation did not significantly attenuate the head movement. For these analyses, all acceleration and velocity traces were aligned on head onset. A one-tailed *t-test*, modified to account for unequal variances in the control and stimulation trials (Milton and Arnold 1995), was applied to compute a P-value for each 2-msec increment. The goal was to determine whether and when (relative to head onset) the head velocity in the stimulation trials was significantly attenuated. A significant attenuation in the head velocity and acceleration for at least 25 ms consecutively was required to count as a valid stimulation effect. The criterion of $P<0.05$ was used for statistical significance across all tests.

RESULTS

Microstimulation was delivered to 23 sites within the OPN region of two monkeys (n=13, monkey *CH*; n=10, monkey *BE*) performing head-unrestrained gaze shifts. The stimulation was either delivered prior to movement initiation or triggered on the onset of the gaze shift. Data were sorted into six target configurations: rightward 40° and 60° gaze shifts initiated from the left hemifield (-20°), leftward 40° and 60° shifts from the right hemifield (20°), leftward gaze shifts (pooled 40° and 48°) from straight-ahead (0°), and rightward gaze shifts (pooled 40°and 48°) from straight-ahead (0°). The six target configurations and two stimulation modes (before and after gaze onset) produced a

maximum of 12 different datasets to be analyzed for each stimulation site. After imposing the constraint that at least 6 trials must exist in each condition, 115 datasets were available for analysis: 48 for stimulation before gaze onset and 67 for stimulation after gaze onset. The eyes were approximately centered in the orbits prior to the onset of gaze shifts for control (mean±sd:0.21±1.92°) and both stimulation (0.25±1.82°) conditions. The distributions were not statistically significantly different (rank sum test, $P<0.05$).

The format of the data presentation order is as follows: a qualitative assessment of the effects of stimulation of the OPN region based on temporal profiles of gaze, head, and eye-in-head signals; an examination of whether and how stimulation modified the latencies of the head and gaze components; an investigation of stimulation-induced alterations in the kinematics and dynamics, with particular emphasis on the head component; an indirect evaluation of the gain of the vestibulo-ocular reflex (VOR) during the stimulation-induced perturbation; and, finally, a brief, statistical consideration of effects of biomechanical factors in addition to that of the stimulation.

Effects of OPN stimulation

Figure 1 illustrates the effects of stimulation of the OPN region on generation of leftward, 40° gaze shifts; the displayed trials are a subset of one dataset. Horizontal amplitude (left column) and velocity (right column) of gaze, head and eye-in-head components are plotted as a function of time for individual control (cyan) and stimulation trials (red). To visualize the effects of stimulation delivered prior to gaze onset (Fig. 1-A1), the movements are aligned on the cue to initiate the gaze shift. For control trials, the

average gaze latency was ~250 ms. For the five stimulation trials shown in the figure, stimulation onset was initiated 150 ms after the cue and lasted for 300 ms. The onset of the gaze shift was delayed until after the end of the stimulation train. A head movement, however, was initiated during the stimulation (Fig. 1-A2) but at a longer latency compared to control trials, as judged by a visual comparison of the velocity traces. Gaze remained stable during this period, implying that the eyes counter-rotated in the orbits by the amount of the head movement (Fig 1-A3) and that the vestibulo-ocular reflex (VOR) gain was near unity. After stimulation offset, a gaze shift composed of an eye saccade and a reaccelerated head movement occurred. Gaze accuracy was maintained as the difference in the total gaze amplitude between control and stimulation conditions was small (stimulation-control, median: -1.08°; mean±sd: -1.19±1.96°) across the 48 datasets. In contrast, the total head movement was greater in the stimulation condition (stimulation-control, median: 1.06°; mean±sd: 1.56±3.05°; $P<0.01$, signrank test), and the reacceleration likely contributed to the hypermetria.

Figure 1 near here

Example movements for which stimulation was triggered on the onset of gaze shifts are shown in Figure 1B. These traces, obtained from the same animal and stimulation site illustrated in Fig. 1A, are aligned on gaze onset. Microstimulation produced an interruption of the gaze shift (Coble et al. 1994; Paré and Guitton 1998; Sparks et al. 2002) that resembled an interrupted saccade observed when the head is restrained (Keller 1977; King and Fuchs 1977). Shortly after stimulation onset, the ongoing gaze shift stopped in mid-flight (Fig. 1-B1) and gaze position remained constant throughout the stimulation period. Since gaze is the sum of eye-in-head and head-on-

trunk positions when trunk position is fixed, the interruption of the gaze shift must be mediated via one or both of these signals. The head continued to move throughout the stimulation period (Fig. 1-B2), but stimulation stopped the ocular saccade in mid-flight (Fig. 1-B3) and the eyes counter-rotated in the orbits. The constant gaze position during the interruption suggests that the VOR gain was near unity during the interruption, nearly perfectly compensating for the sustained head movement. Following stimulation offset, a resumed gaze shift, composed of a coordinated eye-saccade and a reaccelerated head movement, was observed. Gaze accuracy was maintained since the difference in the total gaze amplitude between control and stimulation conditions was small (control-stimulation, median: -0.51°; mean±sd: -0.61±2.78°) across the 67 datasets. In contrast, the total head movement was greater in the stimulation condition (stimulation-control, median: 3.19°; mean±sd: 3.55±2.90°; $P<0.001$, signrank test), and the reacceleration likely contributed to the hypermetria.

Latency distributions

Figure 2 quantifies the changes in latencies of gaze, head and head relative to gaze when stimulation was delivered prior to a movement. Gaze onset was significantly delayed compared to control trials both within and across all datasets (Fig. 2A; rank sum test, $P<0.05$). The distributions of gaze latency across the 48 datasets between control (mean±sd: 266±30 ms) and stimulation (416±89 ms) were statistically different (rank sum test, $P<0.0001$). Like gaze reaction time, head latency was also delayed by the stimulation, and significantly so in 35/48 datasets (Fig 2B; rank sum test, $P<0.05$). The distributions of head latency across all datasets were statistically different for control

(268±43 ms) and stimulation (359±104 ms) trials (rank sum test, $P<0.0001$). Figure 2C shows the timing of eye-head coordination (head-gaze latencies) was significantly altered by the stimulation in 43/48 datasets. Across all 48 datasets, head onset followed gaze onset by 2±27 ms in the control condition but preceded gaze by 57±40 ms during stimulation trials (rank sum test, $P<0.0001$).

Figure 2 near here

When stimulation was triggered after gaze onset (data not shown), in contrast, the onset times of gaze and head were comparable in the control and stimulation conditions. Across the 67 datasets, the distributions of gaze latency for control (263±30 ms) and stimulation (257±33 ms) conditions were not significantly different. Neither were the distributions of head latency (control: 274±44 ms; stimulation: 268±39 ms) or head-gaze latency (control: 11±27 ms; stimulation: 11±24 ms) ($P>0.2$ for all three rank sum tests).

Displacement measurements

The effect of OPN stimulation on the eye and head components of a gaze shift was first evaluated by performing a displacement analysis. Figure 3A illustrates the method used to compute the stimulation-induced displacements when stimulation was delivered prior to gaze onset. The three panels display schematics of gaze, head and eye-in-head movements as a function of time from one dataset (i.e., they have the same target configuration). All traces are aligned on head onset (leftmost first vertical dashed line at time 0). Each panel shows an averaged control movement (thick cyan traces) and two individual stimulation trials (thin waveforms). The initial component of the stimulation traces are shown in dark blue, but they are switched to red and marked with vertical

dashed lines at the onset of the gaze shift that follows the stimulation. First consider the stimulation trial labeled ①. The duration from head onset to gaze onset is identified as the span between the leftmost and the middle vertical dashed lines, and the change is position during this interval is computed for both the averaged control movement (cyan) and the individual stimulation trial (blue and red). This measurement is performed on gaze, head and eye-in-head channels, as illustrated in the three panels in Fig 3A. This same procedure was then repeated for every stimulation trial. The schematic of the trial labeled ② reveals that the duration from head onset to gaze onset varies between trials and hence so do the displacement measures for both control and stimulation conditions. Thus for each dataset, this procedure yields two distributions (control and stimulation conditions) for gaze displacement, two for head displacement, and two for eye-in-head displacement. Furthermore, the number of elements in each distribution equals the number of stimulation trials in the dataset. The procedure was repeated for each of the 48 datasets.

Figure 3 near here

To generate the summary exhibited in Figure 3B, first consider the control and stimulation distributions for the gaze channel. For each dataset, the mean gaze displacement from the control distribution was plotted as a function of the mean gaze displacement from the stimulation condition (top panel). Thus the summary shows data from 48 datasets for which stimulation was delivered before gaze onset. A sign rank test was also applied to each dataset to determine whether the medians of the matched control and stimulations distributions were significantly different. Datasets showing statistically significant difference are shown as circles and crosses otherwise. The average change in

gaze position across all datasets for control (17.8±10.6°) and stimulation (0.8±0.7°) conditions was significantly different (rank sum test, $P<0.0001$).

The same procedure was then applied to the control and stimulation distributions for head and eye-in-head displacements. The summary data are plotted in the middle and bottom panels of Fig. 3B. The eye-in-head displacement was significantly different between control and stimulation conditions in 47 of 48 datasets. The average change in eye position across all datasets for control (12.5±7.7°) and stimulation (–2.2±1.9°) conditions was significantly different also (rank sum test, $P<0.0001$). In contrast, the change in head position between control and stimulation conditions was significant for only 21 datasets. The distributions of head displacements across all datasets for control (4.7±4.1°) and stimulation (3.1±1.9°) conditions tended toward a statistical significance difference (rank sum test, $P=0.054$). For the 21 datasets that were significantly different, the mean change in head position was 6.7±4.5° for control movements and 3.7±1.5° for stimulation trials, which represents a 38% decrement in the head displacement during the interval of analysis.

A similar approach was taken for the displacement analysis when stimulation was triggered on the onset of gaze shifts. The three panels in Fig. 4A are schematized waveforms of gaze, head and eye positions as a function of time for an average control movement (thick, cyan waveforms) and for two, individual stimulation trials (thin traces) aligned on gaze onset (leftmost first vertical dashed line at time 0). The initial component of the stimulation traces are shown in dark blue, but they are switched to red and marked with vertical dashed lines at the onset of the resumed gaze shift that follows the stimulation-induced interruption in gaze. The change in gaze position across this

epoch was computed for each stimulation trial and the average control movement. Since this duration is different across stimulation trials (see trials labeled ① and ②), the displacements for the control distribution are non-identical values. For each dataset, this procedure produces two distributions that were compared with a sign rank test, as described above. The same analysis was also performed for head and eye displacements. For the eye component, however, if the mean control gaze shift was completed before the end of the interval over which the displacements were measured, then the maximum eye-in-head displacement spanning the gaze shift was used (Fig. 4A, ◊ in bottom panel). Note that the analysis on the eye-in-head component does not compare the ocular saccade amplitudes, but rather the change in eye position during the same intervals over which the head displacements were evaluated (except if the control movement had completed, in which case, we considered the saccade amplitude for the eye-in-head displacement measurement).

Figure 4 near here

Figure 4B compares the mean changes in gaze, head and eye positions in control and stimulation conditions across all datasets. The change in gaze (top panel) was significantly different between control and stimulation trials in 66/67 datasets. The average change in gaze position across all datasets for control (36.2±5.8°) and stimulation (19.7±6.3°) conditions was significantly different (rank sum test, $P<0.0001$). Similarly, the eye position displacement (bottom panel) was significantly different between control and stimulation conditions in 66 datasets. The average change in eye position across all datasets for control (20.4±5.6°) and stimulation (5.2±6.8°) conditions was significantly different also (rank sum test, $P<0.0001$). In contrast, the change in head position between

control and stimulation conditions was significant for only 29 datasets. Unlike the consistent stimulation-induced decrease in gaze and eye displacement, however, the head displacement could either increase (9/29) or decrease (20/29). The distributions of head displacements across all datasets for control (15.6±5.7°) and stimulation (14.6±5.4°) conditions were not statistically different (rank sum test, P=0.26).

Velocity and acceleration measurements

While the displacement analysis showed a profound effect on gaze and eye displacements, it did not yield as convincing a result for the head component when stimulation was triggered prior to gaze shifts (Fig. 3). When stimulation was triggered on gaze onset, the displacement analysis failed to find any significant effect on the head component (Fig. 4). It is possible that an effect might have been obscured because of the larger inertia of the head relative to the eyeball (Zangemeister et al. 1981) and because of an ongoing and perhaps attenuated neuromuscular drive to the head during the OPN stimulation. Hence, we further considered the effect of stimulation on the head movement by analyzing velocity and acceleration profiles for control and stimulation trials. Gaze and eye-in-head waveforms were not considered for this analysis.

Figure 5 plots head velocity, aligned on its onset, as a function of time for individual control (cyan) and stimulation trials (blue/red). Each panel represents trials from one dataset. If the stimulation was delivered prior to gaze onset (Fig. 5A, B), the portion of the head movement that occurred before gaze onset is shown in blue; the remainder of the trial is plotted in red. Note that the duration of the blue trace is equivalent to the interval spanned by the vertical dashed lines in Fig. 3A. When

stimulation was triggered on the onset of gaze shifts (Fig. 5C, D), the head movement component that spans from initial gaze onset to resumption of gaze shift following the interruption is shown in blue, and the rest in red. This duration is equivalent to the period spanned by the vertical dashed lines in Fig. 4A. Figure 6 shows the acceleration profiles of the same trials and in same format as Fig. 5.

Figures 5 & 6 near here

The data illustrated in the top row in Figure 5 & 6 were chosen to provide examples of significant attenuation on the head movement for each stimulation condition, whereas the traces shown in the bottom panel demonstrate cases of no obvious modification from the stimulation. In fact, on some stimulation trials, the head velocity and acceleration was higher compared to control trials. This effect was not consistent across all trials within a given dataset, suggesting that the effect was not specific to a stimulation site or to a target configuration. The effect of stimulation on head movements was quantified by examining the dynamics and kinematics of both velocity and acceleration. For each 2-ms increment throughout the duration of the blue traces in Figure 5 (50 ms before head onset to gaze onset), the instantaneous velocity for control and stimulation movements were compared with a one-tailed *t*-test that was modified to account for potentially unequal variances in the two distributions (Milton and Arnold 1995)(see METHODS). Stimulation delivered prior to gaze onset (48 datasets) significantly lowered head velocity and acceleration in 37 and 32 datasets, respectively. The mean±sd (median) attenuation in head velocity and acceleration occurred 34±35 ms (18 ms) and 32±50 ms (19 ms), respectively, after the onset of the head movement. Stimulation triggered on gaze onset (67 datasets) significantly lowered head velocity and

acceleration in 35 and 23 datasets, respectively. The mean±sd (median) attenuation in head velocity and acceleration occurred 77±54 ms (78 ms) and 75±38 ms (74 ms), respectively, after the onset of the head movement. In general, attenuation in head movements occurred later and was less frequent when stimulation was triggered after gaze onset.

The kinematics analyses on the magnitude and time of peak head velocity was performed in the same way as the displacement analysis. For each stimulation trial, the magnitude and time of peak head velocity was computed over the trace spanned from head onset to gaze onset (dark blue traces in Fig. 5). These values were paired with the measurements obtained over the same interval of the average control movement, and a sign-rank test was applied to compare the medians across paired samples of control and stimulation distributions for each dataset. The identical procedure was then performed on head acceleration traces.

The magnitude of peak head velocity was significantly different between control and stimulation conditions for 34/48 datasets when stimulation delayed gaze onset (Fig. 7A). Across all datasets, the distributions of peak head velocity for control (83.4±46.7 °/s) and stimulation (54.1±30.6 °/s) were significantly different (rank sum test, $P<0.001$), corresponding to ~30% decrement in the peak value under stimulation conditions. The magnitude of peak acceleration was significantly different for 23/48 datasets (Fig. 7B). And, like peak head velocity, the distributions of peak head acceleration for control (1702.3±1021.6 °/s^2) and stimulation (1172.1.1±713.0 °/s^2) were also significantly different (rank sum test, $P=0.002$), reflecting a ~25% attenuation due to the stimulation.

Figure 7 near here

When stimulation was triggered on gaze onset, 30 of 67 datasets showed a significant modulation in the peak head velocity measure (Fig. 7C). In a few cases, the stimulation significantly increased peak head velocity. Across all datasets, however, the change was quite small, less than 4% attenuation, and the distributions in control (121.0±58.4 °/s) and stimulation (110.1±52.7 °/s) conditions were not significantly different (rank sum test, $P>0.2$). For peak head acceleration (Fig. 7D), only 15 datasets showed a significant change. Like peak velocity, the stimulation barely reduced peak acceleration, by less than 2%, and there was no statistical difference between the control (2173.7.1.1±1898.8 °/s^2) and stimulation (2019.8±1816.2 °/s^2) distributions (rank sum test, $P>0.4$).

Caution is required when comparing the times of peak velocity and acceleration between control and stimulation conditions. An examination of the temporal profiles in Figs. 5 & 6 reveals why this is the case. When stimulation delayed gaze onset (Fig. 5A, 6A), the head movement was accelerating when the gaze shift was initiated. In other words, the time of peak head velocity (and acceleration) is approximately equal to the duration of the head-only movement (each blue trace). Now note that the cyan, control waveforms across the same interval are also increasing, which implies that the peak times will be very similar for the matched pairs between control and stimulation trials. To circumvent this confound, we appended to each stimulation trial, the 100 ms of data following gaze onset, i.e., 100 ms after each blue trace ends, and computed the peak time measure. We also performed this operation on the datasets collected when stimulation was triggered on gaze onset, although this problem was not common for the long duration stimulation-induced interruptions.

The time of peak head velocity was significantly different for 27/48 datasets when stimulation was delivered before gaze onset (Fig. 8A). Across the datasets, the distributions of control (132±20 ms) and stimulation (159±34 ms) conditions were significantly different (rank sum test, $P<0.0001$). The mean±sd stimulation-induced shift in time to peak velocity was 27±33 ms across the datasets. There was a significant effect in the peak acceleration time for 26 datasets (Fig. 8B). Across all datasets, the distributions of control (80±30 ms) and stimulation (112±36 ms) conditions were significantly different (rank sum test, $P<0.0001$). The mean±sd shift in time was 33±36 ms across the datasets.

Figure 8 near here

Stimulation triggered on the onset of gaze shifts delayed the time of peak head velocity in 36 datasets (Fig. 8C). Across the 67 datasets, the distributions of control (140±27 ms) and stimulation (189±87 ms) conditions were significantly different (rank sum test, $P<0.001$), and the mean±sd stimulation-induced shift in time was 48±77 ms. There was a similar, significant effect in the peak acceleration time for 25 datasets (Fig. 8D). Across all datasets, the distributions of control (85±37 ms) and stimulation (124±81 ms) conditions were significantly different (rank sum test, $P<0.01$). Stimulation delayed the peak time by 39±80 ms across the datasets.

Counter-rotation gain during the interruption

The examples and analyses of Figs. 1, 3A, and 4A demonstrate qualitatively that gaze position remains nearly constant during all stimulation-induced interruptions. Since the head continues to move during this period, the eyes must counter-rotate in the orbits by

the amount of the head movement. We quantified this observation by plotting for each dataset the average change in eye position as a function of the mean head displacement over a period from head onset to gaze onset when stimulation was delivered prior to gaze onset (Fig. 9A). This interval is marked by the vertical dashed lines in Fig. 3A. When stimulation was triggered on gaze onset, the mean changes in eye and head positions during the interval between initial gaze shift offset and resumed gaze shift onset were compared (Fig. 9B). Note that this interval is *not* identical to the duration marked by the vertical lines in Fig. 4A. For both stimulation conditions, the points fall along the negative unity slope (dashed) line.

Figure 9 near here

We quantified this observation with a counter-rotation gain parameter that was computed as the negative of ratio of the eye and head displacements plotted in Fig. 9. This approach of computing the counter-rotation gain is an indirect way to evaluate the VOR gain, which is typically computed as the negative of the ratio of eye and head velocities (Leigh and Zee 1999). A gain close to one would imply that the VOR is fully active. When stimulation was delivered before gaze onset, the mean±sd (median) gain was 0.70±0.27 (0.75). Similarly, when stimulation was triggered after gaze onset, the mean±sd (median) gain was 0.85±0.21 (0.91). Next, we subtracted the magnitudes of eye and head displacements during the counter-rotation phase for each dataset and used a sign rank test to determine whether the median difference across all datasets was significantly different from zero ($P>0.1$, stimulation before gaze onset; $P>0.8$, stimulation after gaze onset). Thus, these results indicate the eye-in-head and head displacements during the counter-rotation were roughly equal in magnitude and opposite in direction, and imply

that the VOR gain is close to unity during the interruption produced by stimulation of the OPN region.

Effects of biomechanical factors

Both the length of a muscle and its velocity of contraction constrain the force generated by a skeletal muscle. Since our experiments required different initial head positions (either roughly centered on the body or deviated approximately 20° to the right or left) and different head dynamics (40° or 60° gaze shifts), we sought to determine whether these parameters could account for the effects observed during OPN stimulation. Unfortunately, head velocity profiles associated with the same initial head position and same desired gaze shift did not display enough variability to test for a combined effect of muscle length and velocity of contraction. Hence, we tested for effects of these parameters separately.

To investigate for a potential effect of head position on the kinematics, we performed a two-way ANOVA with factors initial head position (centered or deviated) and trial type (control or stimulation). Table 1 lists the P-values for the parameters reported in the preceding sections. Consistent with the previous study (Corneil et al. 2001), initial head position influenced most parameters associated with head movements during both stimulation conditions. Note, however, that the effects of the two factors were mostly independent. There were no statistically significant interaction effects when stimulation was delivered prior to gaze onset. When the stimulation was triggered on gaze onset, significant interactions were noted only on the times of peak head velocity and acceleration (Fig. 8) and on the amplitudes of gaze and eye displacements (Fig. 4B).

Tables 1 & 2 near here

To test for an effect of head velocity, we sought to study gaze shifts of very different amplitudes generated from the same initial head position. Our reasoning was that head movements, and therefore head velocities, associated with these gaze shifts are different enough to be considered for statistical (ANOVA) testing. Thus, we only considered trials with desired gaze shifts of 40° and 60° and initial head position at 20° contraversive to the direction of the movement. We performed a two-way ANOVA with factors desired gaze shift (40° and 60°) and trial type (control or stimulation). Table 2 lists the P-values for the parameters reported in the preceding sections. Consistent with the initial head position effect, the desired gaze amplitude – and by extension, head velocity – and the trial type significantly influenced head movement parameters such as displacement, and magnitude and time of peak velocity and acceleration, but there were no interaction effects on the head component.

DISCUSSION

Converging lines of evidence indicate that at least two partially independent pathways are involved in the neural control of coordinated eye and head movements, and that different modes of active eye-head coordination exist. A series of early influential studies (Bizzi et al. 1972; Bizzi et al. 1971) demonstrated that the relative timing of the eye and head components and the patterns of neck muscle activity observed when directing gaze to an unexpected stimulus (triggered mode) is quite different from that observed when animals look to anticipated targets (predictive mode). In general, the onset of the eye and head components are more tightly coupled in the triggered mode, but the head can often lead

for large gaze shifts in the predictive mode (Bizzi et al. 1972; Moschner and Zangemeister 1993; Zangemeister and Stark 1982a). Behavioral paradigms designed to specify separate gaze and head movement goals (Goossens and Van Opstal 1997) and tasks using auditory stimuli (Populin 2006; Tollin et al. 2005) have also demonstrated that the eye and head components of the coordinated movement can achieve a degree of independence.

The results of our OPN stimulation experiments support the partially independent pathways hypothesis, as they demonstrate a dissociation of the eye and head components of gaze shifts, even those produced in the triggered mode. We found that stimulation of the OPN region before gaze onset typically delays the saccadic eye movement until stimulation offset, on the order of several hundred milliseconds, without preventing the head movement (Fig. 2A-C). Triggering the stimulation on the onset of the gaze shift arrests the ongoing saccadic eye movement without stopping the head movement. Furthermore, the duration of the head movement is quite different from the durations of the saccadic eye component and the gaze shift (data not shown, but qualitatively obvious). With early stimulation, for example, the head begins before gaze (and eye saccade) onset and continues after the gaze shift (and eye saccade) terminated.

The *partial* aspect of the partially independent pathways must be emphasized, however, as evidence for interactions between the two pathways are also present in our data. For example, although head movements are not prevented during stimulation delivered before gaze onset, they are significantly delayed (35/48 datasets). There is also a small effect on head amplitude when stimulation is delivered prior to gaze onset (significant for 21/48 datasets) and even when stimulation is triggered on gaze onset

(significant for 29/67 datasets). Moreover, stimulation modified both the initial and peak velocity and acceleration of the head movements in a majority of the datasets. But note that for some datasets, the head kinematics and/or dynamics are greater in the stimulation condition compared to control trials. This effect is not likely specific to a stimulation site or to the target configuration because the enhancement was observed on only some trials within individual datasets (see Fig. 5B, for example). Finally, the ongoing head movement reaccelerates in association with the gaze shift and eye saccade that follows stimulation offset (Fig. 1; also see (Corneil et al. 2002)). Evidence for interactions between the two pathways comes for other studies as well. For instance, natural or stimulation-induced variability in an ongoing head movement dynamics alters the dynamics of the saccadic eye movement (Freedman and Quessy 2004; Freedman and Sparks 2000).

Biomechanical factors (see Tables 1 & 2), such initial head position, velocity of ongoing head movements and inertia could also have contributed to the variability observed in the head dynamics. Despite the variability in the head movement dynamics after OPN stimulation, there was no obvious sign of a sharp deceleration of the head movement. If the OPN stimulation had activated fibers projecting to the antagonistic neck muscles, which are lengthening during an ongoing head movement, then the force produced by the recruitment of lengthening muscle fibers would have been magnified. This would have produced a sharp and observable deceleration, and perhaps even halted the head movement. In our datasets, the deceleration was modest at best, suggesting that stimulation of the OPNs did not result in active breaking of the head movement.

Based on these results, we conclude that stimulation of the OPN region gates the neural pathway required to produce the saccadic eye component of the gaze shift and that this pathway is *not* the only one involved in generating the head component of the gaze shift. This interpretation is in agreement with existing hypotheses of neural control of gaze shifts (Corneil et al. 2002; Freedman 2001; Goossens and Van Opstal 1997; Grantyn and Berthoz 1987; Guitton et al. 1990; Phillips et al. 1995). Figure 10 illustrates a schematic of the pathways and neural commands hypothesized to produce coordinated eye-head movements. It emphasizes that the pathway generating the eye component relies on a desired gaze displacement command (ΔG_d) and is gated by the OPNs. The drive to the neck muscles, in contrast, is a *combination* of a pure head movement command (H_c; pathway 1) and some formulation of ΔG_d. Evidence supporting the notion of a head movement command, not necessarily associated with a gaze shift, comes from neural recordings in the superior colliculus (Gandhi and Walton 2006), central mesencephalic reticular formation (Pathmanathan et al. 2006a,b), microstimulation of the frontal and supplementary eye fields (Chen 2006; Chen and Walton 2005), and adaptation of eye-head coordination in the context of a limited visual field (Constantin et al. 2004). Neural signals encoding a desired gaze displacement command have been proposed to exist at the level of the superior colliculus (Freedman and Sparks 1997a; Freedman et al. 1996; Klier et al. 2001; Munoz et al. 1991), frontal eye field (Guitton and Mandl 1978; Knight and Fuchs 2007; Tu and Keating 2000)(but see (Chen 2006) for an alternative hypothesis), and supplementary eye field (Chen and Walton 2005; Martinez-Trujillo et al. 2003). The ΔG_d command, perhaps after some processing that incorporates the effect of the eye position in the orbits and the location of the stimulus (Freedman

2001), adds to the neck muscle drive at the level of the pontine burst generator (BG). Some studies have suggested that the gaze command drive is parsed into individual, but not necessarily independent, anatomical pathways encoding eye and head movements before BG (pathway 2, Fig. 10; (Freedman 2001; Freedman and Quessy 2004; Phillips et al. 1995)), whereas others have suggested that the separation occurs after BG (pathway 3)(Corneil et al. 2002; Galiana and Guitton 1992; Goossens and Van Opstal 1997; Grantyn et al. 1987; Guitton et al. 1990). These latter two options need not be mutually exclusive. While anatomical support for tectospinal and tectoreticulospinal projections have been reported in cats (Grantyn and Berthoz 1988; Grantyn et al. 1992; Grantyn et al. 1987; Isa and Naito 1995) and monkeys (Cowie et al. 1994; May and Porter 1992; Scudder et al. 1996a; b), it is not known whether they are subject to OPN inhibition.

Figure 10 near here

The interpretations of our OPN stimulation results on the neck muscle drive pathways are limited because of at least two unknown factors: the functional importance of the H_c pathway during gaze shifts, and the effects of OPN stimulation on the H_c and ΔG_d signals. The contribution of the head movement command pathway and how it is affected by OPN stimulation are not known and require further investigation. If the H_c contribution is significant, then our results cannot distinguish between pathways 2 & 3. The occasional observation that head velocity is higher during the stimulation-induced interruption (Fig. 7) implicates a functionally significant role for the H_c command. On the other hand, if the H_c contribution is small or negligible, then our results – in particular, the observation that OPN stimulation does not prevent head movements – provide strong support for a drive to the neck muscles that is not gated by the OPNs

(pathway 2). Pathway 3 also remains viable because numerous head movement characteristics of some datasets were altered, although this effect could also be explained by the effects of OPN stimulation on the ΔG_d command. When head-restrained saccades are interrupted in mid-flight by stimulation of the OPN region, the high-frequency activity in colliculus neurons, presumably those encoding ΔG_d, is suppressed immediately (Keller and Edelman 1994; Keller et al. 2000). The stereotypical saccade-related burst neuron remains quiescent during most of the interruption period and, depending on the interruption duration, the same or another at a more rostral site discharges a high-frequency burst just before the resumed saccade. In another subset of neurons, presumably the buildup type, the low-frequency activity resumes after the initial suppression and maintains a low discharge rate during the interrupted period. Given the colliculus' role in gaze control, it seems safe to assume that these neurons behave similarly for OPNs stimulation during head-unrestrained gaze shifts and head-restrained saccades. Accordingly, we speculate that for stimulation of the OPN region before gaze (or saccade) onset, a subset of collicular neurons will exhibit a low firing rate, but that the level of activity may be attenuated and its onset may be delayed. If this activity represents an attenuated and delayed neuromuscular drive to the neck muscles, the resulting head movement is likely to exhibit a longer onset time and slower dynamics (Fig. 2B). Similarly, when OPN stimulation interrupts ongoing gaze shifts, the immediate suppression followed by low-frequency activity is interpreted as a weaker drive to the neck muscles, resulting in a slower but still continuing head movement. Following stimulation offset, superior colliculus neurons produce a high frequency burst

to generate a gaze shift. This activity also contributes to the neck muscle drive via either pathway (2 or 3) and re-accelerates the ongoing head movement.

Feedback mechanisms

In most models of the saccadic system, feedback control of head-restrained saccades is maintained by subtracting an internal feedback signal representing current eye displacement from a motor command of desired eye displacement (Becker et al. 1981; Robinson 1975). The resulting motor error signal drives the burst generator until feedback reduces it to zero. When the head is unrestrained, appropriate feedback analyses need to consider three signals – gaze, head and eye-in-head. One class of models proposes that the feedback mechanisms preserve gaze accuracy (see review by (Guitton et al. 2003)). This is accomplished by computing a gaze motor error signal as the difference between desired gaze displacement and feedback signals of instantaneous eye-in-head and head displacements (Galiana and Guitton 1992; Guitton et al. 1990). Note that the exact eye and head contributions to the gaze shift are not controlled in this schema. Another family of models suggests that the desired gaze displacement is decomposed into appropriate desired head amplitude and desired eye saccade amplitude, and the feedback mechanism serves the eye pathway only (Freedman 2001; Freedman and Quessy 2004). Gaze and head amplitudes are not controlled in this framework. These competing hypotheses have been tested by observing behavioral and electrophysiological compensation to passive head perturbations (Choi and Guitton 2006; Coimbra et al. 2000; Matsuo et al. 2004; Sylvestre and Cullen 2006), microstimulation of numerous brain structures (Freedman and Quessy 2004; Pélisson et al. 1995), and

naturally prolonged movements (Bergeron and Guitton 2000; 2002). The majority of studies have demonstrated gaze accuracy (see (Freedman and Quessy 2004) for exception). We induced perturbations by stimulation of the OPN region and also found that the mean difference in total gaze amplitude between the control and stimulation conditions was on the order of 1°. Thus, our data are not inconsistent with the gaze comparator class of models.

To evaluate the eye comparator class of models, we would need to compare the total amplitude of the saccadic eye components in the control and stimulation conditions. This comparison would be justified if we can verify that the desired saccadic eye component is not recomputed during the interruption, and extrapolation of existing electrophysiological experiments on the head-restrained system suggests that this condition may be violated. Referring to the effects of interrupted saccades on SC activity discussed above (Keller and Edelman 1994; Keller et al. 2000), the locus of activity on the SC shifts to a rostral site encoding the smaller resumed saccade when interruption durations are long (>70 ms; Keller, personal communications), which was typical of our data. Assuming that this observation also holds for the head-unrestrained condition, the locus of activity would also shift to a more rostral site for the resumed gaze shift. A new desired gaze displacement command could result in recalculating the desired saccadic component, thereby confounding interpretations of a comparison of the total saccade amplitude in the control and stimulation conditions. Hence this analysis is not reported, and we are unable to test the eye comparator class of models in a straight-forward manner.

Summary

We found that stimulation of the OPN region induces dissociation between the eye and head components of gaze shifts. The ocular saccade is completely inhibited by the stimulation. A head movement can be initiated during the stimulation, and an ongoing head movement continues along its trajectory. Post stimulation offset, the gaze shift resumes as a coordinated eye-head movement and preserves gaze accuracy. A reacceleration of the head movement is typically observed in association with the resumed gaze shift.

Compared to the control condition, head movement dynamics are altered during the stimulation – typically they are attenuated but sometimes enhanced. These results indicate that the signals producing the saccadic eye movement component of a coordinated eye-head gaze shift are not the only commands involved in the generation of the head component of the gaze shift. Additional drives to the neck muscles can stem for the desired gaze displacement command and head movement commands not necessarily associated with gaze shifts. This latter signal could be relayed through other volitionally-recruited pathways projecting to the spinal cord and could account for an increase in head dynamics during the stimulation.

ACKNOWLEDGEMENTS

We thank Dennis Murray for animal care and expert assistance during surgical procedures, Kathy Pearson for software assistance, and Sam Houston for machine shop services. The study was funded by NIH grants EY07009, EY015485, and EY01189.

FIGURE LEGENDS

Figure 1 – Temporal representation of effects of stimulation of the OPN region on head-unrestrained gaze shifts. Horizontal amplitude (left column) and velocity (right column) are plotted as a function of time for rightward gaze shifts directed to a target that was briefly flashed at a 60° eccentricity in tangential coordinates. Several, individual control trials are shown in cyan and stimulation trials are shown in red. *(A1-A3)* Effect of stimulation delivered prior to the onset of gaze shifts. The three panels plot the gaze, head, and eye-in-head components of coordinated eye-head movements. The trials are aligned on target onset. For the 5 stimulation trials shown here, stimulation onset occurred 150 ms after target onset and lasted for 300 ms. *(B1-B3)* Effect of stimulation triggered on the onset of gaze shifts. The three panels plot the gaze, head and eye-in-head components, each aligned on gaze onset, as a function of time. Stimulation was triggered as either gaze or head position left its computer controlled window around the fixation point. Stimulation duration for the illustrated red trials was 200 ms. The two datasets shown in panels *(A, B)* have the same target configuration and were collected from the same stimulation site in one animal. The arrows indicate the reacceleration of head movements that accompany gaze shifts after stimulation offset. Also note that the gaze and eye velocity traces illustrated in this figure do not show the dual-peak modulation reported previously (Freedman and Sparks 2000). We speculate that this effect is most robust during visually-guided movements. The movements illustrated here were performed in the memory-guided task, and the absence of visual information is shown to reduce peak velocity, at least of head-restrained saccades (Edelman and

Goldberg 2003). A preliminary examination of the appropriate data collected in the gap task was comparable to the modulation in movement kinematics (data not shown).

Figure 2 – The effect of stimulation of the OPN region on latency. *(A)* Gaze latency, *(B)* head latency, and *(C)* head-gaze onset times are compared for stimulation vs. control conditions when stimulation was triggered before gaze onset. A negative value of head-gaze latency indicates that the head movement preceded gaze onset. Each point represents a dataset (n=48). Statistically significant datasets (o), based on a rank-sum test ($P<0.05$) are differentiated from non-significant datasets (x). The diagonal dashed lines indicate unity slope.

Figure 3 – Analysis of the change in position observed when stimulation was delivered before gaze onset. *(A)* Schematics of gaze (top), head (middle) and eye-in-head (bottom) for an averaged control gaze shift (thick, cyan traces) and two, individual stimulation trials (thin traces shown in blue and red) from the same dataset. The traces are aligned on head onset (leftmost vertical dashed line). For each of the two illustrations of stimulation trials, the initial component is shown in blue, but is changed to red and also marked by a vertical line at the time of gaze onset (post stimulation offset). The change in gaze, head and eye-in-head positions traversed by the control and each stimulation trial for its designated interval was determined. This method produced two distributions (control and stimulation conditions) of displacements each for gaze, head, and eye-in-head components. Note that the amplitude scale is intentionally omitted because the traces are meant to represent schematics. *(B)* The paired displacement measures for the control and stimulation subsets were averaged for each dataset and compared for gaze (top), head (middle) and eye-in-head (bottom) components. Each point corresponds to one dataset.

Statistically significant datasets (o), based on a sign-rank test ($P<0.05$) are differentiated from non-significant datasets (x). The diagonal dashed lines indicate unity slope.

Figure 4 – Analysis of the change in position observed when stimulation was triggered on gaze onset. *(A)* Schematics of gaze (top), head (middle) and eye-in-head (bottom) for an averaged control gaze shift (thick, cyan traces) and two, individual stimulation trials (thin traces shown in blue and red) from the same dataset. The traces are aligned on gaze onset (leftmost vertical dashed line). For each of the two illustrations of stimulation trials, the initial component is shown in blue, but is changed to red and also marked by a vertical line at the time of resumed gaze shift (post stimulation offset). The change in gaze, head and eye-in-head positions traversed by the control and each stimulation trial for its designated interval was determined. This method yielded two distributions (control and stimulation conditions) of displacements each for gaze, head, and eye-in-head components. *(B)* The paired displacement measures for the control and stimulation subsets were averaged for each dataset and compared for gaze (top), head (middle) and eye-in-head (bottom) components. Each point corresponds to one dataset. Statistically significant datasets (o), based on a sign-rank test ($P<0.05$) are differentiated from non-significant datasets (x). The diagonal dashed lines indicate unity slope.

Figure 5 – Temporal evolution of horizontal head velocity. Each panel shows control (cyan) and stimulation (red, blue) trials aligned on head onset, marked by the vertical dashed lines. *(A, B)* Data from two datasets for which stimulation was delivered before gaze onset. The component of head movement that preceded gaze onset in each stimulation trace is shown in blue; this epoch corresponds to the interval marked by the vertical dashed lines in Fig. 3A. The remainder of the trial is shown in red. *(C, D)* Data

from two datasets for which stimulation was triggered on gaze onset. For each stimulation trial, the interval from initial gaze onset to resumed gaze onset is overlaid in blue; the rest of each trial is shown in red. These datasets were chosen to illustrate cases where stimulation did (top panels) and did not (bottom panels) attenuate the head movement.

Figure 6 – Temporal evolution of horizontal head acceleration during control and stimulation conditions. The datasets and figure format are the same as in Figure 5.

Figure 7 – A comparison of peak head velocity *(A, C)* and peak head acceleration *(B, D)* in the control and stimulation conditions. The peak value was computed across the 'blue' component of each stimulation trace (Figs. 5 & 6) and the same interval of an averaged control movement. The control and stimulation values for each dataset were averaged and compared across all datasets. Thus, each point corresponds to one dataset. Statistically significant datasets (o), based on a sign-rank test ($P<0.05$) are differentiated from non-significant datasets (x). The diagonal dashed lines indicate unity slope. Data in left and rights columns represent the conditions when stimulation was delivered before and after gaze onset, respectively.

Figure 8 – A comparison of the times of peak head velocity *(A, C)* and peak head acceleration *(B, D)*. The figure has the same format as Figure 7, but with one major exception. The times of the peak magnitudes were determined over the duration of the blue trials (Figs. 5 & 6) plus another 100 ms (see text for details).

Figure 9 – An indirect evaluation of the counter-rotation gain, which presumably reflects the VOR gain, was assessed by comparing the change in eye position as a function of the head displacement traversed during the stimulation-induced interruption in gaze. *(A)*

When stimulation was delivered before gaze onset, the changes in eye-in-head and head-in-space positions were measured over the interval from head onset to gaze onset (the region marked by the vertical dashed lines in Fig. 3A). *(B)* When stimulation was triggered on gaze onset, the measurements were made across the interval starting at the end of the initial gaze shift and ending at the onset of the resumed gaze shift. Each point represents the average changes in eye and head positions for each dataset.

Figure 10 – Simplified schematic of the flow of neural signals involved in generating coordinated eye-head movements. Two partially independent pathways provide input signals. A head movement command (H_c) provides one drive to the neck muscles (pathway 1), but the functional importance of this pathway during gaze shifts has yet to be determined. A desired gaze displacement command (ΔG_d) contributes to producing the saccadic eye and head components of the gaze shift. One possibility (pathway 2) is that ΔG_d is dissociated into separate eye and head commands *before* the burst generator (BG), which in turn provides a drive to only the extraocular motoneurons (MN_e). Thus, no subset of the ΔG_d drive to the neck muscles is gated by the omnipause neurons (OPN). Another scenario (pathway 3) is that the separation of ΔG_d into separate eye and head pathways occurs *after* the burst generator elements. Note that pathways 2 & 3 need not be mutually exclusive. Abbreviations: BG, burst generator; MN_e, extraocular motoneurons; MN_n, neck motoneurons; OPN, omnipause neurons; ΔG_d, desired gaze displacement command; H_c, head movement command.

REFERENCES

Becker W. Saccades. In: *Eye Movements*, edited by Carpenter RHS. London: The Macmillan Press Ltd, 1991, p. 95-137.

Becker W, and Jürgens R. Gaze saccades to visual targets: does head movement change the metrics. In: *The Head-Neck Sensory Motor System*, edited by Berthoz A, Graf W, and Vidal PP. New York: Oxford Univ. Press, 1992, p. 427-433.

Becker W, King WM, Fuchs AF, Jürgens R, Johanson G, and Kornhuber HH. Accuracy of goal-directed saccades and mechanisms of error correction. In: *Progress in Oculomotor Research*, edited by Fuchs AF, and Becker W. New York: Elsevier, 1981, p. 29-37.

Bergeron A, and Guitton D. Fixation neurons in the superior colliculus encode distance between current and desired gaze positions. *Nat Neurosci* 3: 932-939, 2000.

Bergeron A, and Guitton D. In multiple-step gaze shifts: omnipause (OPNs) and collicular fixation neurons encode gaze position error; OPNs gate saccades. *J Neurophysiol* 88: 1726-1742, 2002.

Bizzi E, Kalil RE, and Morasso P. Two modes of active eye-head coordination in monkeys. *Brain Res* 40: 45-48, 1972.

Bizzi E, Kalil RE, and Tagliasco V. Eye-head coordination in monkeys: Evidence for centrally patterned organization. *Science* 173: 452-454, 1971.

Chen LL. Head movements evoked by electrical stimulation in the frontal eye field of the monkey: evidence for independent eye and head control. *J Neurophysiol* 95: 3528-3542, 2006.

Chen LL, and Walton MM. Head movement evoked by electrical stimulation in the supplementary eye field of the rhesus monkey. *J Neurophysiol* 94: 4502-4519, 2005.

Choi WY, and Guitton D. Responses of collicular fixation neurons to gaze shift perturbations in head-unrestrained monkey reveal gaze feedback control. *Neuron* 50: 491-505, 2006.

Coble ET, Ling L, Phillips JO, and Fuchs AF. The role of omnipause neurons during gaze shifts. In: *Visual and Oculomotor Functions: Advances in Eye Movement Research*, edited by d'Ydewalle G, and Van Resnbergen J. Amsterdam: Elsevier, 1994, p. 285-293.

Cohen B, and Komatsuzaki A. Eye movements induced by stimulation of the pontine reticular formation: evidence for integration in oculomotor pathways. *Exp Neurol* 36: 101-117, 1972.

Cohen YE, and Andersen RA. A common reference frame for movement plans in the posterior parietal cortex. *Nat Rev Neurosci* 3: 553-562, 2002.

Coimbra AJ, Lefèvre P, Missal M, and Olivier E. Difference between visually and electrically evoked gaze saccades disclosed by altering the head moment of inertia. *J Neurophysiol* 83: 1103-1107, 2000.

Constantin AG, Wang H, and Crawford JD. Role of superior colliculus in adaptive eye-head coordination during gaze shifts. *J Neurophysiol* 92: 2168-2184, 2004.

Constantin AG, Wang H, Martinez Trujillo JC, and Crawford DJ. A quantitative comparison of head-free gaze shifts evoked through electrical stimulation of the lateral intraparietal area (LIP) and the superior colliculus (SC) in the macaque. *Soc Neurosci Abstr* Program No. 139.5: 2006.

Corneil BD, Olivier E, and Munoz DP. Neck muscle activity evoked by stimulation of the monkey superior colliculus. II. Relationships with gaze shift initiation and comparison to volitional head movements. *J Neurophysiol* 88: 2000-2018, 2002.
Corneil BD, Olivier E, Richmond FJ, Loeb GE, and Munoz DP. Neck muscles in the rhesus monkey. II. Electromyographic patterns of activation underlying postures and movements. *J Neurophysiol* 86: 1729-1749, 2001.
Courjon JH, Olivier E, and Pelisson D. Direct evidence for the contribution of the superior colliculus in the control of visually guided reaching movements in the cat. *J Physiol* 556: 675-681, 2004.
Cowie RJ, Smith MK, and Robinson DL. Subcortical contributions to head movements in macaques. II. Connections of a medial pontomedullary head-movement region. *J Neurophysiol* 72: 2665-2682, 1994.
Crawford JD, Martinez-Trujillo JC, and Klier EM. Neural control of three-dimensional eye and head movements. *Curr Opin Neurobiol* 13: 655-662, 2003.
Crawford JD, Medendorp WP, and Marotta JJ. Spatial transformations for eye-hand coordination. *J Neurophysiol* 92: 10-19, 2004.
Curthoys IS, Markham CH, and Furuya N. Direct projection of pause neurons to nystagmus-related excitatory burst neurons in the cat pontine reticular formation. *Exp Neurol* 83: 414-422, 1984.
Edelman JA, and Goldberg ME. Saccade-related activity in the primate superior colliculus depends on the presence of local landmarks at the saccade endpoint. *J Neurophysiol* 90: 1728-1736, 2003.
Freedman EG. Interactions between eye and head control signals can account for movement kinematics. *Biol Cybern* 84: 453-462, 2001.
Freedman EG, and Quessy S. Electrical stimulation of rhesus monkey nucleus reticularis gigantocellularis. II. Effects on metrics and kinematics of ongoing gaze shifts to visual targets. *Exp Brain Res* 156: 357-376, 2004.
Freedman EG, and Sparks DL. Activity of cells in the deeper layers of the superior colliculus of the rhesus monkey: evidence for a gaze displacement command. *J Neurophysiol* 78: 1669-1690, 1997a.
Freedman EG, and Sparks DL. Coordination of the eyes and head: movement kinematics. *Exp Brain Res* 131: 22-32, 2000.
Freedman EG, and Sparks DL. Eye-head coordination during head-unrestrained gaze shifts in rhesus monkeys. *J Neurophysiol* 77: 2328-2348, 1997b.
Freedman EG, Stanford TR, and Sparks DL. Combined eye-head gaze shifts produced by electrical stimulation of the superior colliculus in rhesus monkeys. *J Neurophysiol* 76: 927-952, 1996.
Fukushima K, Yamanobe T, Shinmei Y, Fukushima J, Kurkin S, and Peterson BW. Coding of smooth eye movements in three-dimensional space by frontal cortex. *Nature* 419: 157-162., 2002.
Fuller JH. Eye position and target amplitude effects on human visual saccadic latencies. *Exp Brain Res* 109: 457-466, 1996.
Galiana HL, and Guitton D. Central organization and modeling of eye-head coordination during orienting gaze shifts. *Ann N Y Acad Sci* 656: 452-471, 1992.

Gandhi NJ, and Keller EL. Activity of the brain stem omnipause neurons during saccades perturbed by stimulation of the primate superior colliculus. *J Neurophysiol* 82: 3254-3267, 1999.
Gandhi NJ, and Sparks DL. Accuracy of head-unrestrained gaze shifts interrupted by stimulation of the omnipause neurons in monkey. *Soc Neurosci Abstr* 784.783, 2001a.
Gandhi NJ, and Sparks DL. Experimental control of eye and head positions prior to head-unrestrained gaze shifts in monkey. *Vision Res* 41: 3243-3254, 2001b.
Gandhi NJ, and Sparks DL. Microstimulation of the pontine reticular formation in monkey: effects on coordinated eye-head movements. *Soc Neurosci Abstr* 109.108, 2000.
Gandhi NJ, and Walton MM. Superior colliculus activity associated with head movements. *Soc Neurosci Abstr* Program No. 211.2: 2006.
Gardner JL, and Lisberger SG. Linked target selection for saccadic and smooth pursuit eye movements. *J Neurosci* 21: 2075-2084, 2001.
Goffart L, Quinet J, Chavane F, and Masson GS. Influence of background illumination on fixation and visually guided saccades in the rhesus monkey. *Vision Res* 46: 149-162, 2006.
Goossens HH, and Van Opstal AJ. Human eye-head coordination in two dimensions under different sensorimotor conditions. *Exp Brain Res* 114: 542-560, 1997.
Grantyn A, and Berthoz A. Reticulo-spinal neurons participating in the control of synergic eye and head movements during orienting in the cat. I. Behavioral properties. *Exp Brain Res* 66: 339-354, 1987.
Grantyn A, and Berthoz A. The role of the tectoreticulospinal system in the control of head movement. In: *Control of Head Movement*, edited by Peterson BW, and Richmond FJ. New York: Oxford University Press, 1988, p. 224-244.
Grantyn A, Berthoz A, Hardy O, and Gourdon A. Contribution of reticulospinal neurons to the dynamic control of head movements: presumed neck bursters. In: *The Head-Neck Sensory-Motor System*, edited by Berthoz A, Vidal PP, and Graf W. New York: Oxford, 1992, p. 318-329.
Grantyn A, Ong-Meang Jacques V, and Berthoz A. Reticulo-spinal neurons participating in the control of synergic eye and head movements during orienting in the cat. II. Morphological properties as revealed by intra-axonal injections of horseradish peroxidase. *Exp Brain Res* 66: 355-377, 1987.
Graziano MS, Hu XT, and Gross CG. Coding the locations of objects in the dark [see comments]. *Science* 277: 239-241, 1997.
Guitton D, Bergeron A, Choi WY, and Matsuo S. On the feedback control of orienting gaze shifts made with eye and head movements. *Prog Brain Res* 142: 55-68, 2003.
Guitton D, and Mandl G. Frontal 'oculomotor' area in alert cat. II. Unit discharges associated with eye movements and neck muscle activity. *Brain Res* 149: 313-327, 1978.
Guitton D, Munoz DP, and Galiana HL. Gaze control in the cat: studies and modeling of the coupling between orienting eye and head movements in different behavioral tasks. *J Neurophysiol* 64: 509-531, 1990.
Huebner WP, Paloski WH, Reschke MF, and Bloomberg JJ. Geometric adjustments to account for eye eccentricity in processing horizontal and vertical eye and head movement data. *J Vestib Res* 5: 299-322, 1995.

Isa T, and Naito K. Activity of neurons in the medial pontomedullary reticular formation during orienting movements in alert head-free cats. *J Neurophysiol* 74: 73-95, 1995.
Keller EL. Control of saccadic eye movements by midline brain stem neurons. In: *Control of Gaze by Brain Stem Neurons*, edited by Baker R, and Berthoz A. Amsterdam: Elsevier, 1977, p. 327-336.
Keller EL, and Edelman JA. Use of interrupted saccade paradigm to study spatial and temporal dynamics of saccadic burst cells in superior colliculus in monkey. *J Neurophysiol* 72: 2754-2770, 1994.
Keller EL, Gandhi NJ, and Vijay Sekaran S. Activity in deep intermediate layer collicular neurons during interrupted saccades. *Exp Brain Res* 130: 227-237, 2000.
Keller EL, Gandhi NJ, and Weir PT. Discharge of superior collicular neurons during saccades made to moving targets. *J Neurophysiol* 76: 3573-3577, 1996.
King WM, and Fuchs AF. Neuronal activity in the mesencephalon related to vertical eye movements. In: *Control of Gaze by Brain Stem Neurons*, edited by Baker R, and Berthoz A. Amsterdam: Elsevier, 1977, p. 319-326.
Klier EM, Wang H, and Crawford JD. The superior colliculus encodes gaze commands in retinal coordinates. *Nat Neurosci* 4: 627-632, 2001.
Knight TA, and Fuchs AF. Contribution of the frontal eye field to gaze shifts in the head-unrestrained monkey: effects of microstimulation. *J Neurophysiol* 97: 618-634, 2007.
Land MF. Predictable eye-head coordination during driving. *Nature* 359: 318-320, 1992.
Land MF, and McLeod P. From eye movements to actions: how batsmen hit the ball. *Nat Neurosci* 3: 1340-1345, 2000.
Leigh RJ, and Zee DS. *The Neurology of Eye Movements*. New York: Oxford University Press, 1999, p. 643.
Martinez-Trujillo JC, Wang H, and Crawford DJ. Electrical stimulation of the supplementary eye fields in the head-free macaque evokes kinematically normal gaze shifts. *J Neurophysiol* 89: 2961-2974, 2003.
Matsuo S, Bergeron A, and Guitton D. Evidence for gaze feedback to the cat superior colliculus: discharges reflect gaze trajectory perturbations. *J Neurosci* 24: 2760-2773, 2004.
May PJ, and Porter JD. The laminar distribution of macaque tectobulbar and tectospinal neurons. *Vis Neurosci* 8: 257-276, 1992.
Milton JS, and Arnold JC. *Introduction to probability and statistics: principles and applications for engineering and the computing sciences*. New York: McGraw-Hill, Inc., 1995, p. 811.
Moschner C, and Zangemeister WH. Preview control of gaze saccades: efficacy of prediction modulates eye-head interaction during human gaze saccades. *Neurol Res* 15: 417-432, 1993.
Munoz DP, Guitton D, and Pélisson D. Control of orienting gaze shifts by the tectoreticulospinal system in the head-free cat. III. Spatiotemporal characteristics of phasic motor discharges. *J Neurophysiol* 66: 1642-1666, 1991.
Paré M, and Guitton D. Brain stem omnipause neurons and the control of combined eye-head gaze saccades in the alert cat. *J Neurophysiol* 79: 3060-3076, 1998.

Pathmanathan J, Cromer J, Cullen K, and Waitzman D. Temporal characteristics of neurons in the central mesencephalic reticular formation of head unrestrained monkeys. *Exp Brain Res* 1, 2005a.
Pathmanathan J, Presnell R, Cromer J, Cullen K, and Waitzman D. Spatial characteristics of neurons in the central mesencephalic reticular formation (cMRF) of head-unrestrained monkeys. *Exp Brain Res* 1, 2005b.
Pélisson D, Goffart L, and Guillaume A. Control of saccadic eye movements and combined eye/head gaze shifts by the medio-posterior cerebellum. *Prog Brain Res* 142: 69-89, 2003.
Pélisson D, Goffart L, Guillaume A, Catz N, and Raboyeau G. Early head movements elicited by visual stimuli or collicular electrical stimulation in the cat. *Vision Res* 41: 3283-3294, 2001.
Pélisson D, Guitton D, and Goffart L. On-line compensation of gaze shifts perturbed by micro-stimulation of the superior colliculus in the cat with unrestrained head. *Exp Brain Res* 106: 196-204, 1995.
Phillips JO, Ling L, Fuchs AF, Siebold C, and Plorde JJ. Rapid horizontal gaze movement in the monkey. *J Neurophysiol* 73: 1632-1652, 1995.
Populin LC. Monkey sound localization: head-restrained versus head-unrestrained orienting. *J Neurosci* 26: 9820-9832, 2006.
Quinet J, and Goffart L. Saccade dysmetria in head-unrestrained gaze shifts after muscimol inactivation of the caudal fastigial nucleus in the monkey. *J Neurophysiol* 93: 2343-2349, 2005.
Robinson DA. Oculomotor control signals. In: *Basic Mechanisms of Ocular Motility and Their Clinical Implications*, edited by Bach-y-Rita P, and Lennerstrand G. Oxford: Pergamon, 1975, p. 337-374.
Scudder CA, Moschovakis AK, Karabelas AB, and Highstein SM. Anatomy and physiology of saccadic long-lead burst neurons recorded in the alert squirrel monkey. I. Descending projections from the mesencephalon. *J Neurophysiol* 76: 332-352, 1996a.
Scudder CA, Moschovakis AK, Karabelas AB, and Highstein SM. Anatomy and physiology of saccadic long-lead burst neurons recorded in the alert squirrel monkey. II. Pontine neurons. *J Neurophysiol* 76: 353-370, 1996b.
Sparks DL, Barton EJ, Gandhi NJ, and Nelson J. Studies of the role of the paramedian pontine reticular formation in the control of head-restrained and head-unrestrained gaze shifts. *Ann NY Acad Sci* 956: 85-98, 2002.
Sparks DL, Freedman EG, Chen LL, and Gandhi NJ. Cortical and subcortical contributions to coordinated eye and head movements. *Vision Res* 41: 3295-3305, 2001.
Sparks DL, and Gandhi NJ. Single cell signals: an oculomotor perspective. *Prog Brain Res* 142: 35-53, 2003.
Stuphorn V, Bauswein E, and Hoffmann KP. Neurons in the primate superior colliculus coding for arm movements in gaze-related coordinates. *J Neurophysiol* 83: 1283-1299, 2000.
Sylvestre PA, and Cullen KE. Premotor correlates of integrated feedback control for eye-head gaze shifts. *J Neurosci* 26: 4922-4929, 2006.
Tollin DJ, Populin LC, Moore JM, Ruhland JL, and Yin TC. Sound-localization performance in the cat: the effect of restraining the head. *J Neurophysiol* 93: 1223-1234, 2005.

Tu TA, and Keating EG. Electrical stimulation of the frontal eye field in a monkey produces combined eye and head movements. *J Neurophysiol* 84: 1103-1106, 2000.
Walton MM, and Gandhi NJ. The role of superior colliculus in the control of head movements: effects of reversible inactivation. *Soc Neurosci Abstr* Program No. 211.3: 2006.
Walton MMG, and Mays LE. Discharge of saccade-related superior colliculus neurons during saccades accompanied by vergence. *J Neurophysiol* 90: 1124-1139, 2003.
White JM, Sparks DL, and Stanford TR. Saccades to remembered target locations: an analysis of systematic and variable errors. *Vision Res* 34: 79-92, 1994.
Zangemeister WH, Lehman S, and Stark L. Simulation of head movement trajectories: model and fit to main sequence. *Biol Cybern* 41: 19-32, 1981.
Zangemeister WH, and Stark L. Gaze latency: variable interactions of head and eye latency. *Exp Neurol* 75: 389-406, 1982a.
Zangemeister WH, and Stark L. Types of gaze movement: variable interactions of eye and head movements. *Exp Neurol* 77: 563-577, 1982b.

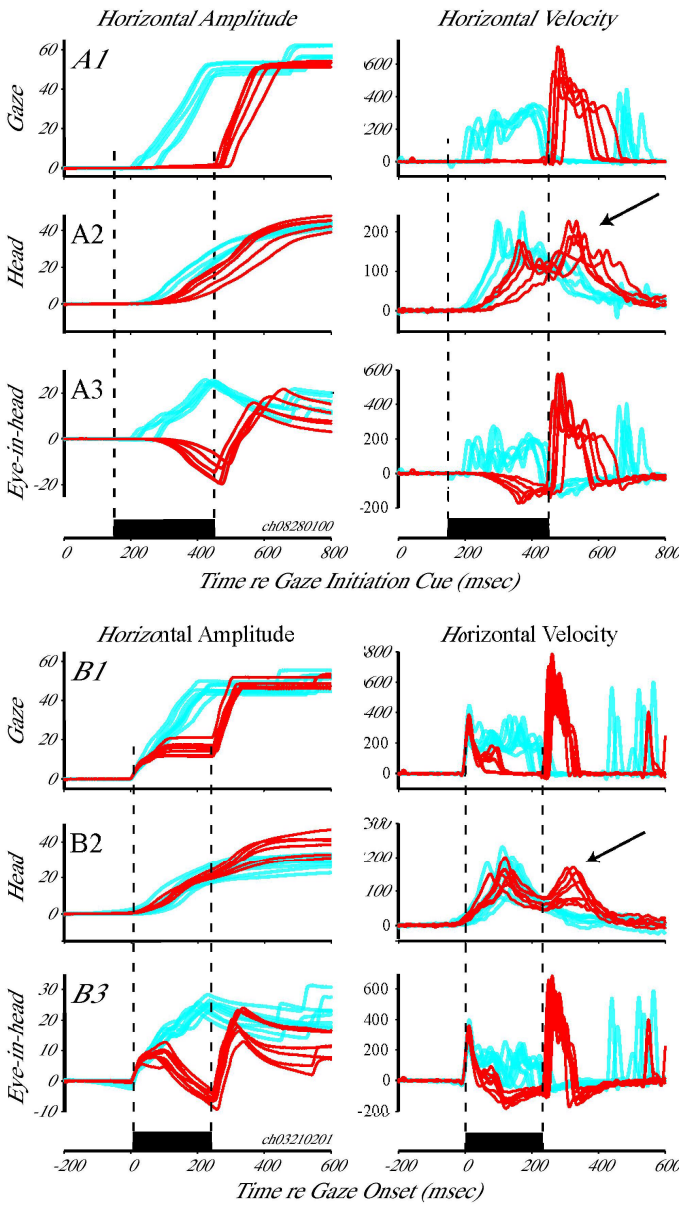

Figure 1 - Temporal representation of effects of stimulation of the OPN region on head-unrestrained gaze shifts. Horizontal amplitude (left column) and velocity (right column) are plotted as a function of time for rightward gaze shifts directed to a target that was briefly flashed at a 60° eccentricity in tangential coordinates. Several, individual control trials are shown in cyan and stimulation trials are shown in red. (A1-A3) Effect of stimulation delivered prior to the onset of gaze shifts. The three panels plot the gaze, head, and eye-in-head components of coordinated eye-head movements. The trials are aligned on target onset. For the 5 stimulation trials shown here, stimulation onset occurred 150 ms after target onset and lasted for 300 ms. (B1-B3) Effect of stimulation triggered on the onset of gaze shifts. The three panels plot the gaze, head and eye-in-head components, each aligned on gaze onset, as a function of time. Stimulation was triggered as either gaze or head position left its computer controlled window around the fixation point. Stimulation duration for the illustrated red trials was 200 ms. The two

datasets shown in panels (A, B) have the same target configuration and were collected from the same stimulation site in one animal. The arrows indicate the reacceleration of head movements that accompany gaze shifts after stimulation offset. Also note that the gaze and eye velocity traces illustrated in this figure do not show the dual-peak modulation reported previously (Freedman and Sparks 2000). We speculate that this effect is most robust during visually-guided movements. The movements illustrated here were performed in the memory-guided task, and the absence of visual information is shown to reduce peak velocity, at least of head-restrained saccades (Edelman and Goldberg 2003). A preliminary examination of the appropriate data collected in the gap task was comparable to the modulation in movement kinematics (data not shown).

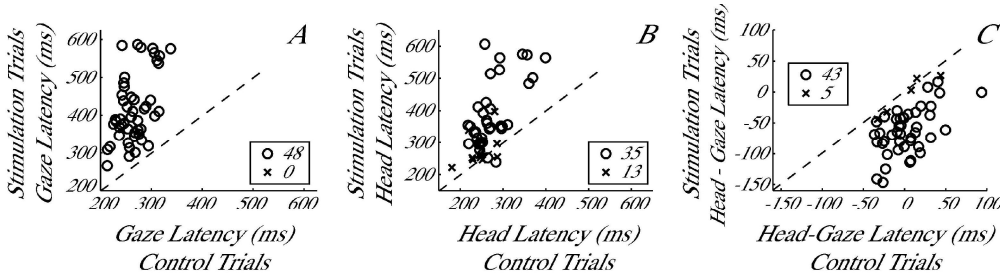

Figure 2 - The effect of stimulation of the OPN region on latency. (A) Gaze latency, (B) head latency, and (C) head-gaze onset times are compared for stimulation vs. control conditions when stimulation was triggered before gaze onset. A negative value of head-gaze latency indicates that the head movement preceded gaze onset. Each point represents a dataset (n=48). Statistically significant datasets (o), based on a rank-sum test (P<0.05) are differentiated from non-significant datasets (x). The diagonal dashed lines indicate unity slope.

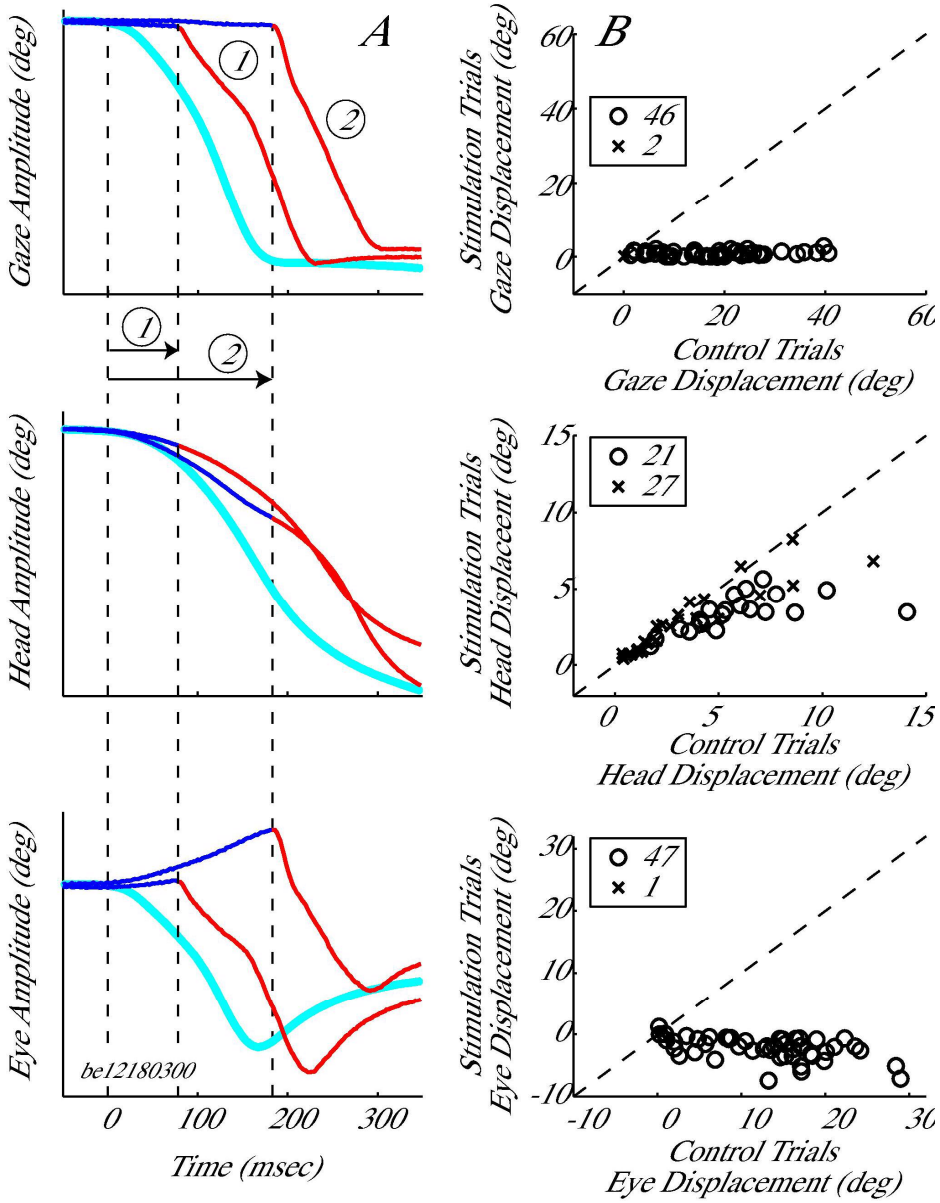

Figure 3 - Analysis of the change in position observed when stimulation was delivered before gaze onset. (A) Schematics of gaze (top), head (middle) and eye-in-head (bottom) for an averaged control gaze shift (thick, cyan traces) and two, individual stimulation trials (thin traces shown in blue and red) from the same dataset. The traces are aligned on head onset (leftmost vertical dashed line). For each of the two illustrations of stimulation trials, the initial component is shown in blue, but is changed to red and also marked by a vertical line at the time of gaze onset (post stimulation offset). The change in gaze, head and eye-in-head positions traversed by the control and each stimulation trial for its designated interval was determined. This method produced two distributions (control and stimulation conditions) of displacements each for gaze, head, and eye-in-head components. Note that the amplitude scale is intentionally omitted because the traces are meant to represent schematics. (B) The paired displacement measures for the

control and stimulation subsets were averaged for each dataset and compared for gaze (top), head (middle) and eye-in-head (bottom) components. Each point corresponds to one dataset. Statistically significant datasets (o), based on a sign-rank test (P<0.05) are differentiated from non-significant datasets (x). The diagonal dashed lines indicate unity slope.

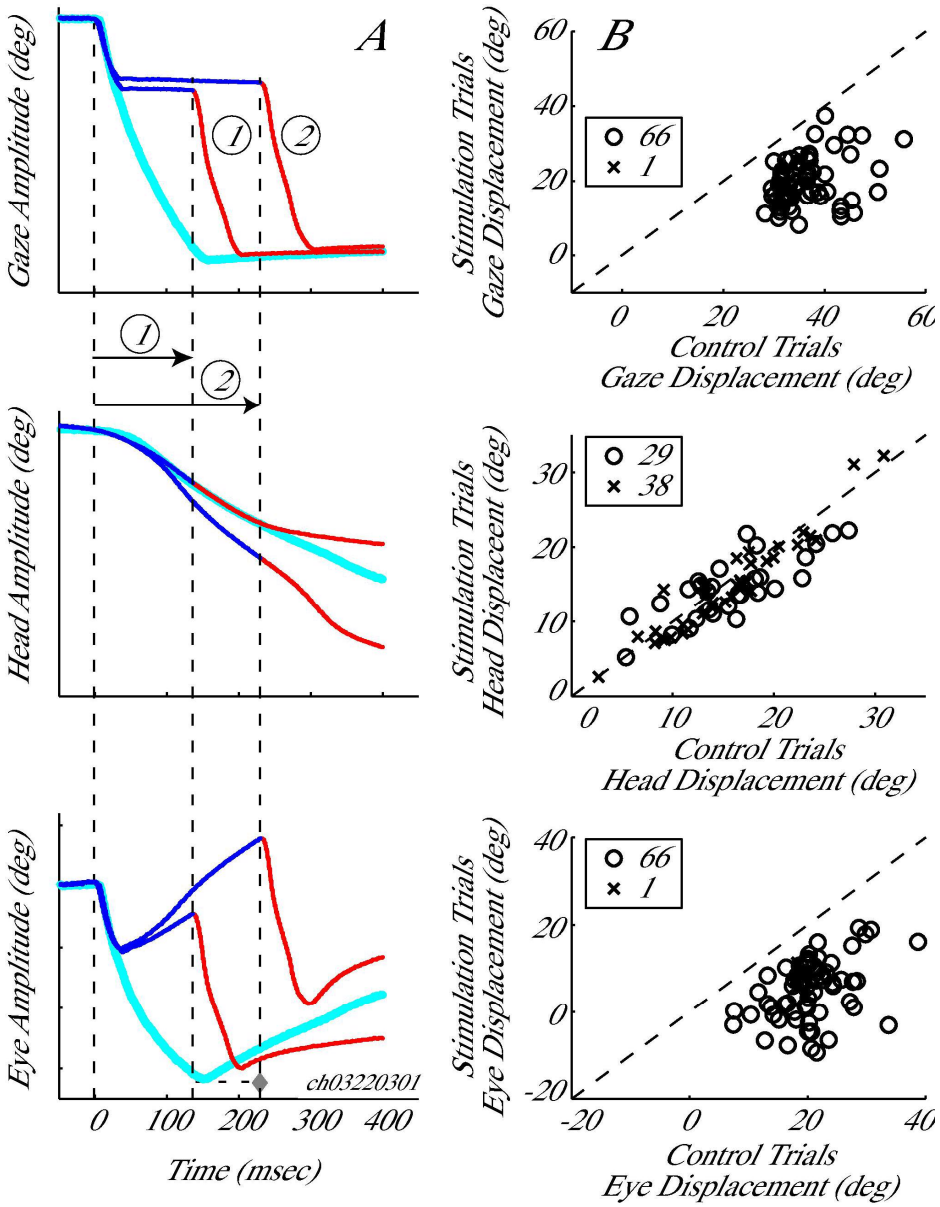

Figure 4 - Analysis of the change in position observed when stimulation was triggered on gaze onset. (A) Schematics of gaze (top), head (middle) and eye-in-head (bottom) for an averaged control gaze shift (thick, cyan traces) and two, individual stimulation trials (thin traces shown in blue and red) from the same dataset. The traces are aligned on gaze onset (leftmost vertical dashed line). For each of the two illustrations of stimulation trials, the initial component is shown in blue, but is changed to red and also marked by a vertical line at the time of resumed gaze shift (post stimulation offset). The change in gaze, head and eye-in-head positions traversed by the control and each stimulation trial for its designated interval was determined. This method yielded two distributions (control and stimulation conditions) of displacements each for gaze, head, and eye-in-head components. (B) The paired displacement measures for the control and stimulation subsets were averaged for each dataset and compared for gaze (top), head (middle) and

eye-in-head (bottom) components. Each point corresponds to one dataset. Statistically significant datasets (o), based on a sign-rank test (P<0.05) are differentiated from non-significant datasets (x). The diagonal dashed lines indicate unity slope.

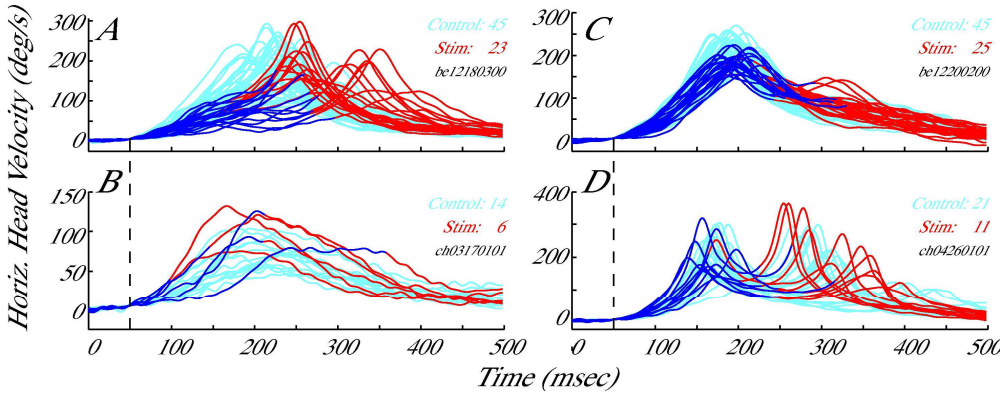

Figure 5 - Temporal evolution of horizontal head velocity. Each panel shows control (cyan) and stimulation (red, blue) trials aligned on head onset, marked by the vertical dashed lines. (A, B) Data from two datasets for which stimulation was delivered before gaze onset. The component of head movement that preceded gaze onset in each stimulation trace is shown in blue; this epoch corresponds to the interval marked by the vertical dashed lines in Fig. 3A. The remainder of the trial is shown in red. (C, D) Data from two datasets for which stimulation was triggered on gaze onset. For each stimulation trial, the interval from initial gaze onset to resumed gaze onset is overlaid in blue; the rest of each trial is shown in red. These datasets were chosen to illustrate cases where stimulation did (top panels) and did not (bottom panels) attenuate the head movement.

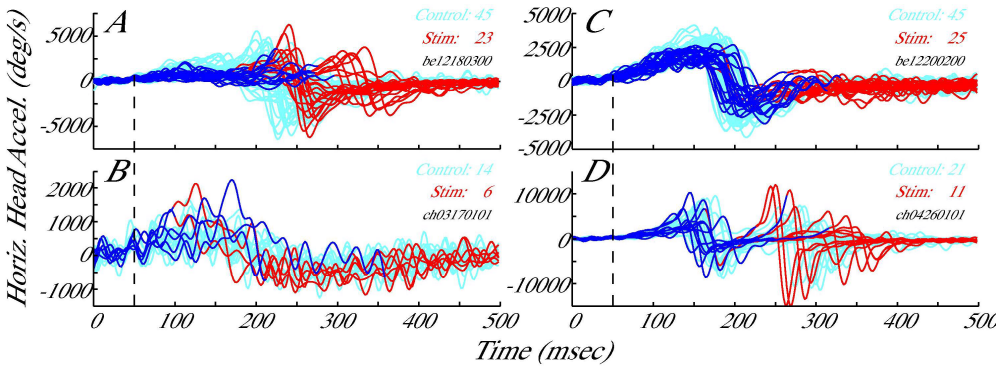

Figure 6 - Temporal evolution of horizontal head acceleration during control and stimulation conditions. The datasets and figure format are the same as in Figure 5.

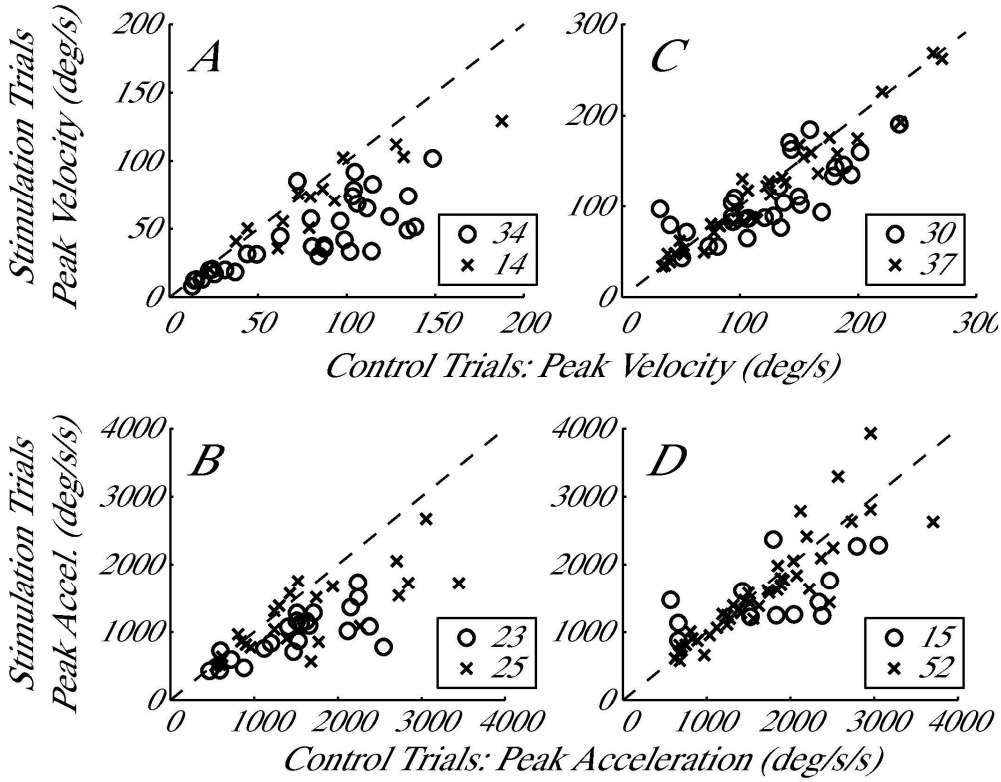

Figure 7 - A comparison of peak head velocity (A, C) and peak head acceleration (B, D) in the control and stimulation conditions. The peak value was computed across the 'blue' component of each stimulation trace (Figs. 5 & 6) and the same interval of an averaged control movement. The control and stimulation values for each dataset were averaged and compared across all datasets. Thus, each point corresponds to one dataset. Statistically significant datasets (o), based on a sign-rank test (P<0.05) are differentiated from non-significant datasets (x). The diagonal dashed lines indicate unity slope. Data in left and rights columns represent the conditions when stimulation was delivered before and after gaze onset, respectively.

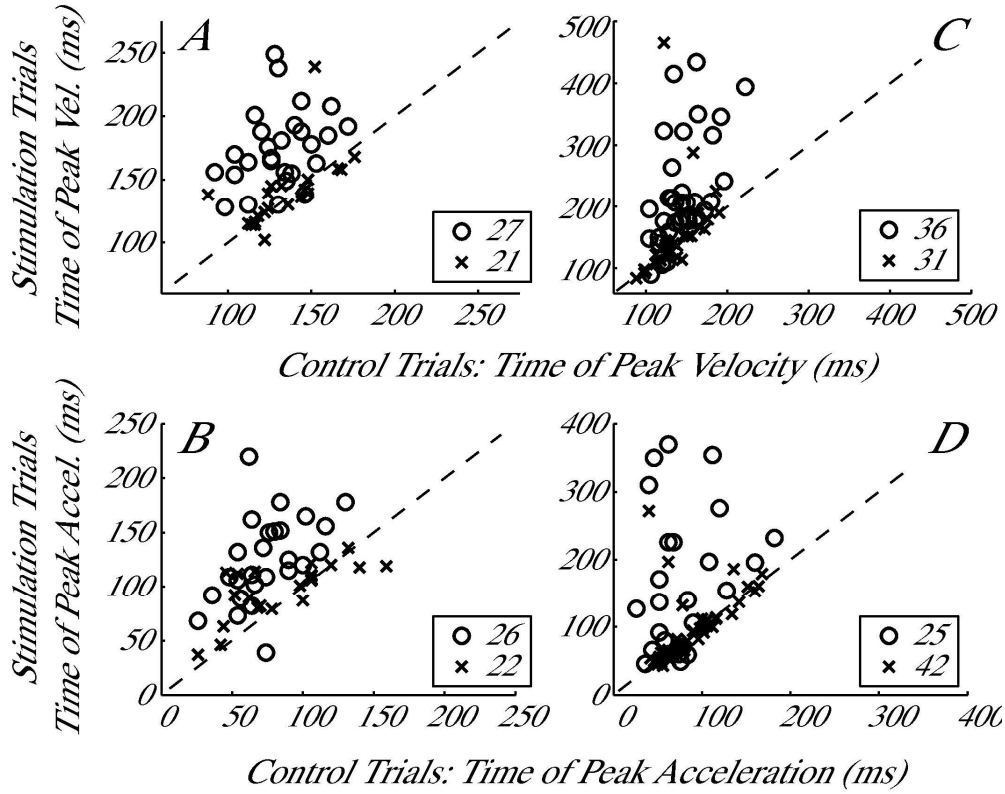

Figure 8 - A comparison of the times of peak head velocity (A, C) and peak head acceleration (B, D). The figure has the same format as Figure 7, but with one major exception. The times of the peak magnitudes were determined over the duration of the blue trials (Figs. 5 & 6) plus another 100 ms (see text for details).

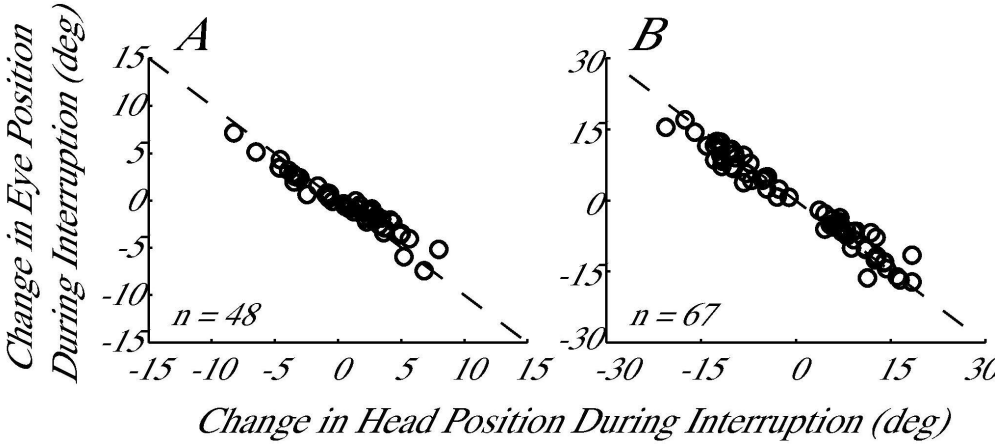

Figure 9 - An indirect evaluation of the counter-rotation gain, which presumably reflects the VOR gain, was assessed by comparing the change in eye position as a function of the head displacement traversed during the stimulation-induced interruption in gaze. (A) When stimulation was delivered before gaze onset, the changes in eye-in-head and head-in-space positions were measured over the interval from head onset to gaze onset (the region marked by the vertical dashed lines in Fig. 3A). (B) When stimulation was triggered on gaze onset, the measurements were made across the interval starting at the end of the initial gaze shift and ending at the onset of the resumed gaze shift. Each point represents the average changes in eye and head positions for each dataset.

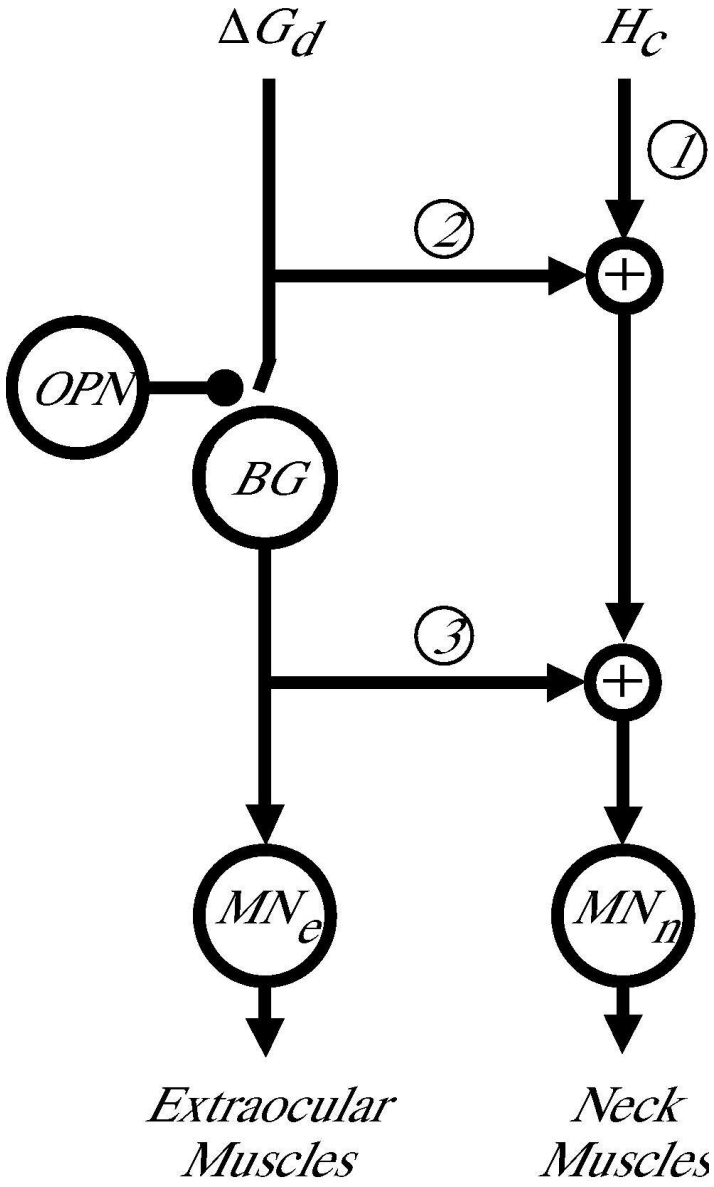

Figure 10 - Simplified schematic of the flow of neural signals involved in generating coordinated eye-head movements. Two partially independent pathways provide input signals. A head movement command (Hc) provides one drive to the neck muscles (pathway 1), but the functional importance of this pathway during gaze shifts has yet to be determined. A desired gaze displacement command (ΔGd) contributes to producing the saccadic eye and head components of the gaze shift. One possibility (pathway 2) is that ΔGd is dissociated into separate eye and head commands before the burst generator (BG), which in turn provides a drive to only the extraocular motoneurons (MNe). Thus, no subset of the ΔGd drive to the neck muscles is gated by the omnipause neurons (OPN). Another scenario (pathway 3) is that the separation of ΔGd into separate eye and head pathways occurs after the burst generator elements. Note that pathways 2 & 3 need not be mutually exclusive. Abbreviations: BG, burst generator; MNe, extraocular

motoneurons; MNn, neck motoneurons; OPN, omnipause neurons; ΔGd, desired gaze displacement command; Hc, head movement command.

Table 1 – P-values obtained from 2-way ANOVA on analyzed parameters. The independent variables were initial head position (IHP; centered or contraversive to gaze shift direction) and trial type (control or stimulation).

	Stimulation *before* gaze onset			Stimulation *after* gaze onset		
Parameter	IHP	TYPE	IHP*TYPE	IHP	TYPE	IHP*TYPE
Gaze latency (Fig. 2A,D)	0.2118	0	0.1394	0.4945	0.2549	0.9663
Head latency (Fig. 2B, E)	0.0039	3.3277E-08	0.0852	0.0006	0.4062	0.8925
Head re gaze onset (Fig. 2C,F)	1.6245E-05	8.3250E-12	0.2811	1.0799E-06	0.9150	0.7711
Gaze displacement (Fig. 3B, 4B)	0.2775	8.4377E-15	0.3924	1.7536E-05	0	0.0277
Head displacement (Fig. 3B, 4B)	0.0007	0.0575	0.4877	4.7184E-14	0.1962	0.8853
Eye displacement (Fig. 3B, 4B)	0.6758	0	0.4453	0.0249	0	0.0427
Peak velocity (Fig. 7A,C)	1.5157E-06	0.0038	0.2439	4.3432E-13	0.1873	0.4207
Peak acceleration (Fig. 7B,D)	3.8370E-05	0.0313	0.1779	1.0530E-05	0.6287	0.7544
Time of peak velocity (Fig. 8A,C)	0.0693	0.0003	0.1679	0.0001	2.7972E-06	0.0078
Time of peak acceleration (Fig. 8B,D)	0.0002	4.5796E-05	0.5252	0.0054	0.0001	0.0006

Table 2 – P-values obtained from 2-way ANOVA on analyzed parameters. The independent variables were desired gaze amplitude (ΔG_d; 40° or 60° desired gaze shift displacement; all movements were initiated from the same initial head position: 20° contraversive to gaze shift direction) and trial type (control or stimulation).

	Stimulation *before* gaze onset			Stimulation *after* gaze onset		
Parameter	ΔG_d	TYPE	ΔG_d*TYPE	ΔG_d	TYPE	ΔG_d*TYPE
Gaze latency (Fig. 2A,D)	0.5291	1.8874E-15	0.9566	0.5624	0.6668	0.9791
Head latency (Fig. 2B, E)	0.7672	1.7405E-06	0.6005	0.6723	0.7650	0.7815
Head re gaze onset (Fig. 2C,F)	0.0473	1.1102E-16	0.2212	0.7792	0.8159	0.6285
Gaze displacement (Fig. 3B, 4B)	0.2827	0	0.3573	3.8325E-05	0	0.0018
Head displacement (Fig. 3B, 4B)	0.0046	0.0162	0.3378	0.0425	0.1663	0.4994
Eye displacement (Fig. 3B, 4B)	0.9055	0	0.4768	0.0253	0	0.0529
Peak velocity (Fig. 7A,C)	0.0111	0.0002	0.3454	2.4101E-06	0.0227	0.3402
Peak acceleration (Fig. 7B,D)	0.0975	0.0058	0.6556	0.0322	0.4568	0.6284
Time of peak velocity (Fig. 8A,C)	0.0070	1.1975E-06	0.1718	0.0011	0.0003	0.2291
Time of peak acceleration (Fig. 8B,D)	0.0002	3.4773E-08	0.0847	0.0001	0.1924	0.1722